NTNU

Norwegian University of
Science and Technology

Spin-orbit coupled multiband superconductors

Gudmund Gunnarsen

MSc in Physics
Submission date: August 2016
Supervisor: Asle Sudbø, IFY

Norwegian University of Science and Technology
Department of Physics

ACKNOWLEDGEMENTS

I would like to thank Prof. Asle Sudbø for being extremely helpful, for putting up with me despite my many shortcomings, and for introducing me to a field that I quickly discovered I had an immense interest in. The conversations I've had with him on the calculations involved in this thesis has been some of the most enjoyable experiences I've had.

A model for square lattice spin orbit coupled cooper pairing is derived using mean field theory. We look at three cases, a magnetic field parallel to the lattice, perpendicular to the lattice, and no magnetic field. For the cases of perpendicular or zero field, the cooper pairs have zero momentum, and we are able to find conditions on the spin-basis BCS interaction under which the system produces chiral p-wave cooper pairing, with gaps of the form $\Delta(\boldsymbol{k}) \sim k_x + ik_y$. For the parallel field case, we compare calculations with those of [1] and find corrections to the helicity basis interactions, and thus the gap equations.

I. INTRODUCTION

In 1957 J. Bardeen, L.N. Cooper, and J.R. Schrieffer introduced what is now known as the BCS model for superconductivity [2]. In this model, fermions on a lattice, outside of the Fermi sea, interact in such a way as to form paired bound states. These paired states called Cooper pairs have associated with them an energy gap, a lower energy level necessary to excite electrons into the state, as well as to break the state apart. This suppresses scattering effects that would lead to e.g. electrical resistance, and if these effects are too weak to affect the pairs, we would get zero electrical resistance and thus superconductivity.

There is a type of superconductor that is described in a different way altogether when compared to ordinary phases of matter. It is called a topological superconductor, and it is joined by some other states such as topological insulators [3–5] and systems with the quantum spin hall effect [6–8], as states that are described by topological order rather than ordinary Landau symmetries. These types of states have in recent years been of high interest [9–11]. Associated with the topological states are integers characterizing whether the states are topologically trivial or not such as the first Chern number [12, 13]. The trivial states are ordinary insulators, superconductors and so on, while the nontrivial ones have special edge states. They are known as topological states as it is not possible to adiabatically deform the energy spectra of the nontrivial states into that of the trivial ones, without edge states.

The edge states, as their names suggest, are located at the boundaries of the system, at interfaces between topologically trivial and nontrivial materials. This interplay between the bulk and the edge of the system that produces these special states is usually referred to as the bulk-boundary correspondence. The edge states are helical, that is they have a connection between spin and momentum, and therefore are referred to as a helical liquid [14]. What causes the boundary to be of interest is the many unique properties that the helical liquid possesses. It can be a gapless liquid, being conductive unlike perhaps the bulk [15]. The helical properties means backscattering is difficult and therefore it is resistant to non-magnetic impurities [16, 17]. Finally, for topological SC, the boundary states can be Majorana fermions [18]. An important point to note here is also that these states are holographic, they appear only on the boundary of the system, and cannot exist without the bulk boundary correspondence. Thus we are not necessarily able to expect finding a similar structure outside of these topological materials.

However, why are these topological materials of actual interest? There are several reasons, ranging from purely theoretical interest to actual practical effects. A rather distant goal concerns quantum computation. Topological quantum computation involves topologically protected q-bits, using topological states such as the fractional quantum hall states [19] and in general quantum computation revolves around usage of holographic Majorana states with non-abelian statistics [20, 21]. In addition, no Majorana fermions have been observed as elementary particles, they are only theorized to appear as quasi-particles in condensed matter systems, such as the topological materials described above. As such, these states are a way to produce and observe Majorana fermions for experimental purposes.

The type of topological superconductor that will be looked into in this thesis is the chiral p-wave superconductor. This type of superconductor has a gap that goes as $\Delta(\boldsymbol{k}) \sim k_x + ik_y$, and it is not TR invariant. The chiral p-wave structure comes from spin orbit coupling (SOC), which is the interaction between the spin and momentum of a particle. Chiral p-wave superconductors are interesting because they allow edge states to appear and are thus topologically non-trivial [18], but they also have interesting effects such as allowing zero energy Majorana quasiparticles inside vortices [22], which further leads to non-abelian statistics of braided vortices [23]. This is for reasons involving decoherence interesting in regards to quantum computing. A physical realization of the chiral p-wave superconductor has been proposed for some materials [24]. There are also proposals for chiral superconductors by using hybrid systems [25]

First, finding conditions for chiral p-wave pairing is what will be done in this thesis. Specifically, the working conditions will be a square lattice of identical ions, with a perpendicular electric field causing Rashba SOC as well

as a Zeeman field causing further band splitting. Under these conditions we will find the requirements on the BCS interaction potential such that the superconductivity is of a chiral p-wave nature.

Secondly, we will study the effects of adding in-plane magnetic fields briefly, and look at specific calculations of interaction terms from an article written by Florian Loder, A. P. Kampf and Thilo Kopp [1]. The in-plane field functions similarly to SOC, but with the important difference of being momentum independent. It will both deform and displace the Fermi surfaces of the system, and we may as a result be dependent on finding a finite-$\boldsymbol{q}$ center of mass momentum for the interaction, unlike the standard case of no in-plane field. There will be a discrepancy between their results and the calculations presented in this thesis.

II. LATTICE HAMILTONIAN

We begin by briefly looking at general interactions between fermions on a 2-dimensional, square lattice of ions. The ions are presumed to be all identical, but kept general as we use purely phenomenological interactions in this model. Each ion contributes one fermion to the overall system, with N ions and thus N fermions. and we have the general form of our Hamiltonian as

$$H = \sum_{i,j,s,\sigma} V_{i,j} c^\dagger_{i,s} c_{j,\sigma} + \sum_{i,j,i',j'} \sum_{s,\sigma,s',\sigma'} V_{i,j,i',j'} c^\dagger_{i,s} c^\dagger_{j,\sigma} c_{i',s'} c_{j',\sigma'}, \tag{1}$$

where i, j, i', j' are points on the lattice while s, σ, s', σ' are spin indices. $V_{i,j}, V_{i,j,i',j'}$ are the potentials, while $c^\dagger, c$ are fermion creation and annihilation operators respectively, and thus satisfy the fermion anti-commutation relations

$$\begin{aligned} \{c^\dagger_{i,s}, c^\dagger_{j,\sigma}\} &= \{c_{i,s}, c_{j,\sigma}\} = 0 \\ \{c^\dagger_{i,s}, c_{j,\sigma}\} &= \delta_{i,j}\delta_{s,\sigma} \end{aligned} \tag{2}$$

In equation (1), we have the first sum as a one-particle interaction term, for instance interaction with external fields, or the lattice itself. The second is a two-particle interaction term. In our particular model, the only two-particle term is the BCS potential itself, while the SOC potential, Zeeman field, in-plane magnetic field interactions and the standard kinetic term are one-particle terms.

A. Kinetic energy terms

As a first calculation, we shall diagonalize the hopping term, or the kinetic energy term. The nearest neighbour hopping term is

$$H_{n.n} = \sum_{<i,j>,s} -t_{i,j} c^\dagger_{i,s} c_{j,s}, \tag{3}$$

with $t_{i,j}$ as the energy value of this hopping from lattice site j to site i, while $< i, j >$ denotes that we are including only nearest neighbours i, j in the sum. It is of interest to transform this expression into momentum space, where the Hamiltonian is diagonal and of a free Fermi gas form. We use the Fourier transformations

$$\begin{aligned} c_{i,s} &= \frac{1}{\sqrt{N}} \sum_{\boldsymbol{k}} e^{-i\boldsymbol{k}\boldsymbol{r}_i} c_{\boldsymbol{k},s} \\ c_{\boldsymbol{k},s} &= \frac{1}{\sqrt{N}} \sum_{i} e^{i\boldsymbol{k}\boldsymbol{r}_i} c_{i,s}, \end{aligned} \tag{4}$$

with N being the number of lattice sites, k the lattice momentum and $\boldsymbol{r}_i$ denoting the position of lattice site i. Inserting this transformation into equation (3):

$$H_{n.n} = \sum_{<i,j>} \sum_{\boldsymbol{k},\boldsymbol{k'},s} e^{i(\boldsymbol{k'}\boldsymbol{r}_j - \boldsymbol{k}\boldsymbol{r}_i)} \frac{-t_{i,j}}{N} c^\dagger_{\boldsymbol{k},s} c_{\boldsymbol{k'},s} \tag{5}$$

In an isotropic lattice of identical ions, $t_{i,j}$ must be a constant for all nearest neighbours i, j, and so it reduces to just t. For nearest neighbours, $\boldsymbol{r}_j = \boldsymbol{r}_i + \boldsymbol{\delta}$, $\boldsymbol{r}_i$ being the position of lattice point i, with $\boldsymbol{\delta}$ as the vectors from one lattice site to the four nearest neighbours. In a square lattice $\boldsymbol{\delta} = \{\pm a\hat{x}, \pm a\hat{y}\}$, with a as the lattice constant, and we rewrite to

$$H_{n.n} = \frac{-t}{N} \sum_{\boldsymbol{k},\boldsymbol{k'},s} \sum_{i,\boldsymbol{\delta}} e^{i(\boldsymbol{k'}-\boldsymbol{k})\boldsymbol{r}_i} e^{i\boldsymbol{k'}\boldsymbol{\delta}} c^\dagger_{\boldsymbol{k},s} c_{\boldsymbol{k'},s}. \tag{6}$$

For a lattice we have $\sum_i e^{i(k'-k)\boldsymbol{r}_i} = \delta_{\boldsymbol{k},\boldsymbol{k'}} N$, and so we reduce to

$$\begin{aligned} H_{n.n} &= -t \sum_{\boldsymbol{k},s} \sum_{\boldsymbol{\delta}} e^{i\boldsymbol{k}\boldsymbol{\delta}} c^\dagger_{\boldsymbol{k},s} c_{\boldsymbol{k},s} \\ &= -t \sum_{\boldsymbol{k},s} (e^{ik_x} + e^{-ik_x} + e^{ik_y} + e^{-ik_y}) c^\dagger_{\boldsymbol{k},s} c_{\boldsymbol{k},s} \\ &= -2t \sum_{\boldsymbol{k},s} (\cos(k_x) + \cos(k_y)) c^\dagger_{\boldsymbol{k},s} c_{\boldsymbol{k},s}, \end{aligned} \tag{7}$$

where we have for convenience absorbed the lattice constant into the momenta k_x, k_y. We now have nearest neighbour terms in diagonal form in momentum space. We could go on to derive the next nearest neighbour term, however it is of little interest in this model, as it does not impact the qualitative results. In [1] the next nearest neighbour interaction is included, and they have the form

$$H_{n.n.n} = 4t' \sum_{\boldsymbol{k},s} \cos(k_x)\cos(k_y) c^\dagger_{\boldsymbol{k},s} c_{\boldsymbol{k},s}, \tag{8}$$

with t' as the interaction strength. Defining now $\epsilon_{\boldsymbol{k}} = -2t(\cos(k_x) + \cos(k_y)) + 4t'\cos(k_x)\cos(k_y)$ we have as kinetic terms

$$H_0 = \sum_{\boldsymbol{k},s} \epsilon_{\boldsymbol{k}} c^\dagger_{\boldsymbol{k},s} c_{\boldsymbol{k},s}. \tag{9}$$

B. Spin orbit coupling terms

There are many ways to introduce spin-orbit coupling into a system of fermions, but in this thesis we are looking at Rashba SOC. This is simply the name for having a perpendicular electric field E on our 2-dimensional lattice. For convenience, we set our lattice to be in the xy-plane, and so the electric field will be along the z-axis. The Rashba SOC term in the Hamiltonian is [26]

$$H_{SOC} = -\sum_i \alpha(\boldsymbol{E} \times \hat{p}_i) \cdot \boldsymbol{\sigma}_i \tag{10}$$

which is just the sum of individual interactions between each fermion and the E-field, for some α as the interaction strength.

We would like to convert this to the convenient second-quantized form, as well as Fourier transform the term into momentum space so we can diagonalize the Hamiltonian once more. The electrical field is simply $\boldsymbol{E} = (0, 0, E) = E \cdot \hat{z}$, and so we simplify to

$$H_{SOC} = \frac{1}{2}\sum_i \alpha E(p_{i,y}\sigma_x - p_{i,x}\sigma_y). \tag{11}$$

p_x and p_y are the momentum or translation operators which in creation and annihilation operators read

$$\begin{aligned} p_{i,x} &= -i(c^\dagger_{\boldsymbol{r}_i} c_{\boldsymbol{r}_i + a\hat{x}} - c^\dagger_{\boldsymbol{r}_i} c_{\boldsymbol{r}_i - a\hat{x}}) \\ p_{i,y} &= -i(c^\dagger_{\boldsymbol{r}_i} c_{\boldsymbol{r}_i + a\hat{y}} - c^\dagger_{\boldsymbol{r}_i} c_{\boldsymbol{r}_i - a\hat{y}}), \end{aligned} \tag{12}$$

where the ordinary i index is changed to $\boldsymbol{r}_i$ for convenience. Using also the Pauli spin matrices

$$\begin{aligned} \sigma_x &= \begin{pmatrix} 0 & 1 \\ 1 & 0 \end{pmatrix} \\ \sigma_y &= \begin{pmatrix} 0 & -i \\ i & 0 \end{pmatrix}, \end{aligned} \tag{13}$$

we insert to get

$$\begin{aligned} H_{SOC} &= \frac{i}{2}\sum_i \sum_{s,s'} A((c^\dagger_{\boldsymbol{r}_i,s} c_{\boldsymbol{r}_i + a\hat{y},s'} - c^\dagger_{\boldsymbol{r}_i,s} c_{\boldsymbol{r}_i - a\hat{y},s'})\sigma_{x,ss'} - (c^\dagger_{\boldsymbol{r}_i,s} c_{\boldsymbol{r}_i + a\hat{x},s'} - c^\dagger_{\boldsymbol{r}_i,s} c_{\boldsymbol{r}_i - a\hat{x},s'})\sigma_{y,ss'}) \\ &= \frac{i}{2}\sum_i \sum_s A((c^\dagger_{\boldsymbol{r}_i,s} c_{\boldsymbol{r}_i + a\hat{y},-s} - c^\dagger_{\boldsymbol{r}_i,s} c_{\boldsymbol{r}_i - a\hat{y},-s}) + i\Gamma_{1s}(c^\dagger_{\boldsymbol{r}_i,s} c_{\boldsymbol{r}_i + a\hat{x},-s} - c^\dagger_{\boldsymbol{r}_i,s} c_{\boldsymbol{r}_i - a\hat{x},-s})), \end{aligned} \tag{14}$$

where we have defined $A = \alpha E$ and

$$\Gamma_{\alpha\beta}\begin{cases} 1 & \text{if } \alpha = \beta \\ -1 & \text{if } \alpha \neq \beta \end{cases}, \tag{15}$$

which for indices with two states is a quantity that is antisymmetric in both indices α, β.

Going to momentum space through Fourier transformation:

$$\begin{aligned} H_{SOC} &= \frac{i}{2N}\sum_i \sum_{\boldsymbol{k},\boldsymbol{k'}} \sum_s A e^{i(\boldsymbol{k'}-\boldsymbol{k})\boldsymbol{r}_i}((e^{i\boldsymbol{k'}a\hat{y}} c^\dagger_{\boldsymbol{k},s} c_{\boldsymbol{k'},-s} - e^{-i\boldsymbol{k'}a\hat{y}} c^\dagger_{\boldsymbol{k},s} c_{\boldsymbol{k'},-s}) + i\Gamma_{1s}(e^{i\boldsymbol{k'}a\hat{x}} c^\dagger_{\boldsymbol{k},s} c_{\boldsymbol{k'},-s} - e^{-i\boldsymbol{k'}a\hat{x}} c^\dagger_{\boldsymbol{k},s} c_{\boldsymbol{k'},-s})) \\ &= \sum_{\boldsymbol{k},s} A(\sin(k_y) + i\Gamma_{1s}\sin(k_x)) c^\dagger_{\boldsymbol{k},s} c_{\boldsymbol{k},-s}, \end{aligned} \tag{16}$$

where on the last line we have also used that

$$2i\sin(v) = e^{iv} - e^{-iv} \tag{17}$$

and

$$\sum_i e^{i(\boldsymbol{k}-\boldsymbol{k'})\boldsymbol{r}_i} = \delta_{\boldsymbol{k},\boldsymbol{k'}} N \tag{18}$$

We finally define

$$A_{\boldsymbol{k},s} = A(\sin(k_y) + i\Gamma_{1s}\sin(k_x)), \tag{19}$$

which corresponds to the energy value of the above interaction. Rewriting:

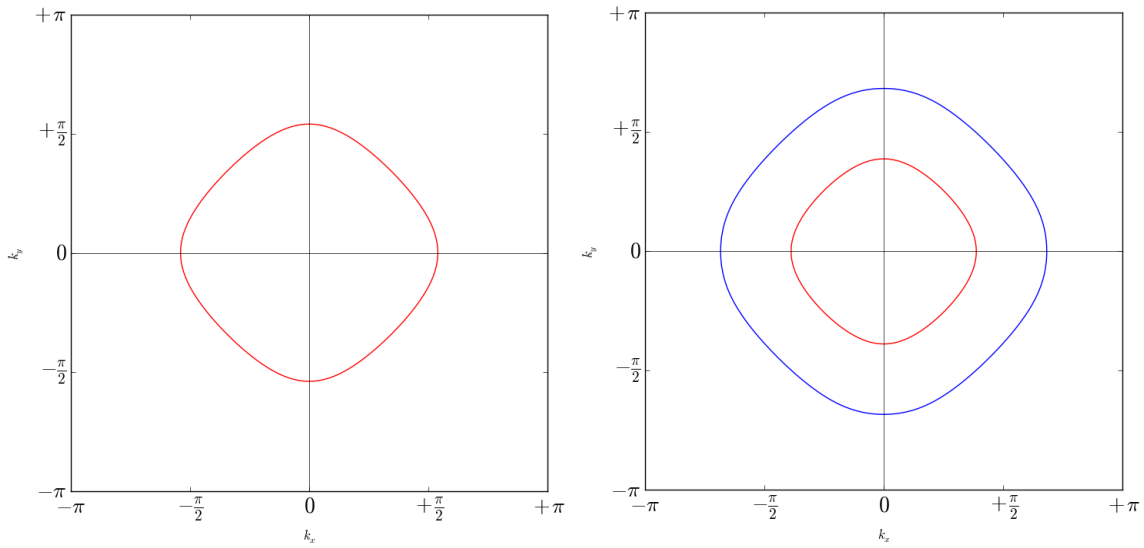

(a) No SOC, one band.

(b) SOC, split bands.

Figure 1: Fermi surfaces, with or without SOC.

$$H_{SOC} = \sum_{\boldsymbol{k},s} A_{\boldsymbol{k},s} c^\dagger_{\boldsymbol{k},s} c_{\boldsymbol{k},-s}. \tag{20}$$

Finally, it will be convenient below to make the definition $A_{\boldsymbol{k}} = A_{\boldsymbol{k},\uparrow}$, because of the fact that $A_{\boldsymbol{k},s} = A^\dagger_{\boldsymbol{k},-s}$.

We now move to diagonalize the total Hamiltonian including the already diagonal kinetic term from equation (9) as well as the new off-diagonal SOC term. In doing this, we will turn to the helicity basis, getting a band index that determines the helicity of each fermion. We combine equations (20) and (9) into a matrix equation,

$$H = \sum_{\boldsymbol{k}} \gamma^\dagger_{\mathbf{k}} \begin{bmatrix} \epsilon_{\boldsymbol{k}} - \mu & A_{\boldsymbol{k}} \\ A^\dagger_{\boldsymbol{k}} & \epsilon_{\boldsymbol{k}} - \mu \end{bmatrix} \gamma_{\mathbf{k}}, \tag{21}$$

where

$$\gamma^\dagger_{\boldsymbol{k}} = (c^\dagger_{\boldsymbol{k},\uparrow}\ c^\dagger_{\boldsymbol{k},\downarrow}). \tag{22}$$

The eigenvalues of the matrix in equation (21) are given by $\lambda^2 - 2(\epsilon_{\boldsymbol{k}} - \mu)\lambda + (\epsilon_{\boldsymbol{k}} - \mu)^2 - |A_{\boldsymbol{k}}|^2 = 0$, which has as solutions

$$E_{\boldsymbol{k},\alpha} = \epsilon_{\boldsymbol{k}} - \mu + \Gamma_{\alpha 1}|A_{\boldsymbol{k}}|. \tag{23}$$

Fermi surfaces of this energy spectrum are plotted in Figure 1, in 1a the surface is plotted for no SOC, while in 2 the SOC has been turned on. The most notable feature is that the band has been split by the presence of SOC. Both bands remain centro-symmetric and concentric however.

In figure 2 we see the whole of the energy spectrum $E_{\boldsymbol{k}}, \alpha$ plotted for 1BZ, showing the overall shape. It is the $E_{\boldsymbol{k}}$-plane slices that are shown above in figure 1, while in this 3 dimensional figure one can see details such as the 4 minima of the lower energy blue band.

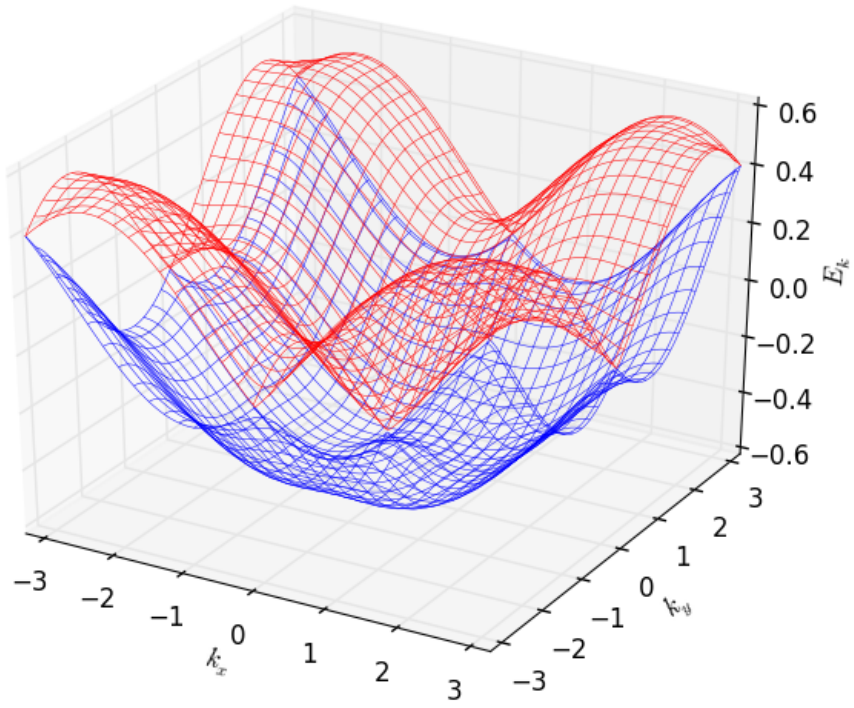

Figure 2: Energy spectra with SOC

Thus, in the helicity basis, we have a new Hamiltonian that reads

$$H = \sum_{\boldsymbol{k},\alpha} E_{\boldsymbol{k},\alpha} a^{\dagger}_{\boldsymbol{k},\alpha} a_{\boldsymbol{k},\alpha}. \tag{24}$$

$a_{\boldsymbol{k},\alpha}$ are the helicity band fermionic operators, but we need to know their exact form expressed as a linear combination of spin fermionic operators. Since H is hermitian, we know that the matrix in (21) must be unitarily diagonalizable. Inserting the eigenvalues (23) into the eigenvalue equation of the matrix in equation (21), we get

$$\begin{bmatrix} \pm|A_{\boldsymbol{k}}| & A_{\boldsymbol{k}} \\ A^{\dagger}_{\boldsymbol{k}} & \pm|A_{\boldsymbol{k}}| \end{bmatrix} \begin{pmatrix} x_1 \\ x_2 \end{pmatrix} = 0 \tag{25}$$

which has as solutions

$$\mathbf{x} = \frac{\mathbf{1}}{\sqrt{\mathbf{2}}} \begin{pmatrix} 1 \\ \pm\Phi^{\dagger}_{\boldsymbol{k}} \end{pmatrix}, \tag{26}$$

where the $\frac{1}{\sqrt{2}}$ is for normalization purposes to keep the transformation unitary, while $\Phi_{\boldsymbol{k}}$ is the phase of $A_{\boldsymbol{k}}$,

$$\Phi_{\boldsymbol{k}} = \frac{A_{\boldsymbol{k}}}{|A_{\boldsymbol{k}}|}. \tag{27}$$

Inserting the transformation matrix

$$P_{\boldsymbol{k}}^{\dagger} = \frac{1}{\sqrt{2}} \begin{bmatrix} 1 & 1 \\ \Phi_{\boldsymbol{k}}^{\dagger} & -\Phi_{\boldsymbol{k}}^{\dagger} \end{bmatrix} \tag{28}$$

as $1 = P_{\boldsymbol{k}}^{\dagger} P_{\boldsymbol{k}}$ into equation (21), we end up with equation (24) in matrix form:

$$H = \sum_{\boldsymbol{k}} (P_{\boldsymbol{k}}\gamma_{\boldsymbol{k}})^{\dagger} (P_{\boldsymbol{k}} \begin{bmatrix} \epsilon_{\boldsymbol{k}} - \mu & A_{\boldsymbol{k}} \\ A_{\boldsymbol{k}}^{\dagger} & \epsilon_{\boldsymbol{k}} - \mu \end{bmatrix} P_{\boldsymbol{k}}^{\dagger})(P_{\boldsymbol{k}}\gamma_{\boldsymbol{k}}) = \sum_{\boldsymbol{k}} \eta_{\boldsymbol{k}}^{\dagger} \begin{bmatrix} E_{\boldsymbol{k},1} & 0 \\ 0 & E_{\boldsymbol{k},2} \end{bmatrix} \eta_{\boldsymbol{k}}, \tag{29}$$

with

$$\eta_{\boldsymbol{k}} = \begin{pmatrix} a_{\boldsymbol{k},1} \\ a_{\boldsymbol{k},2} \end{pmatrix} = P_{\boldsymbol{k}}\gamma_{\boldsymbol{k}} = \frac{1}{\sqrt{2}} \begin{bmatrix} 1 & \Phi_{\boldsymbol{k}} \\ 1 & -\Phi_{\boldsymbol{k}} \end{bmatrix} \begin{pmatrix} c_{\boldsymbol{k},\uparrow} \\ c_{\boldsymbol{k},\downarrow} \end{pmatrix}. \tag{30}$$

We can now write down the transformations directly from equation (30):

$$a_{\boldsymbol{k},\alpha} = \frac{c_{\boldsymbol{k},\uparrow} + \Gamma_{1\alpha}\Phi_{\boldsymbol{k}} c_{\boldsymbol{k},\downarrow}}{\sqrt{2}} \tag{31}$$

The inverse transformations are achieved by setting $P^{\dagger}\eta_{\boldsymbol{k}} = \gamma_{\boldsymbol{k}}$, and read:

$$\begin{aligned} c_{\boldsymbol{k},\uparrow} &= \frac{a_{\boldsymbol{k},1} + a_{\boldsymbol{k},2}}{\sqrt{2}} \\ c_{\boldsymbol{k},\downarrow} &= \Phi_{\boldsymbol{k}}^{\dagger} \frac{a_{\boldsymbol{k},1} - a_{\boldsymbol{k},2}}{\sqrt{2}} \end{aligned} \tag{32}$$

C. In-plane magnetic field

In addition to SOC, we can add an in-plane magnetic field. This field will couple to the spins of the fermions in much the same way as the SOC, however the combination of SOC and in-plane magnetic field significantly alters the problem [27–29]. One should note that the Fermi surfaces are significantly both deformed and displaced from their normal SOC-induced concentric centrosymmetric form with an in-plane magnetic field. This is shown in Figure 3, for weak, equal, and strong in-plane fields relative to the SOC strength. As a result of the combination of in-plane fields and SOC, we can get Fulde-Ferrell [30] Larkin Ovchinnikov [31] states, and this kind of finite momentum state can lead to a topological superconductivity with edge state Majorana fermions [32, 33]. In a recent paper [34] a strong magnetic field weak coupling state for a 2-dimensional electron gas was studied, and below will be calculations of an in-plane only magnetic field, with the limit of weak SOC used to compare the transformations found by Starykh et al. to this square lattice case.

Figure 3 shows Fermi surfaces of this system, with an in-plane magnetic field in the y-direction. Unlike the case in Figure 1 without this magnetic field, the Fermi surfaces are not concentric or centro-symmetric. This means that zero momentum offset $\boldsymbol{q}$ is no longer the best approximation for intraband pairing. Thus we are forced to find finite momenta $\boldsymbol{q}$ to optimize pairing on each band. However even in doing this, there is no perfect choice like $\boldsymbol{q} = 0$ for centro-symmetric surfaces, because the surfaces in this case are not just offset but also deformed.

The magnetic field coupling goes as

$$H_B = \sum_i \mu_B \boldsymbol{B} \cdot \hat{S}_i \tag{33}$$

with $\boldsymbol{B} = B_x\hat{x} + B_y\hat{y}$ as the magnetic field and a constant μ_B determining the strength of the coupling. Using the same notation in general as [1] for convenience and comparison, we set $\mu_B\boldsymbol{B} = H_x\hat{x} + H_y\hat{y}$. We use the spin operator in second quantized form $\hat{S}_i = \sum_{s,s'} \boldsymbol{\sigma}_{ss'} c_{i,s}^{\dagger} c_{i,s'}$

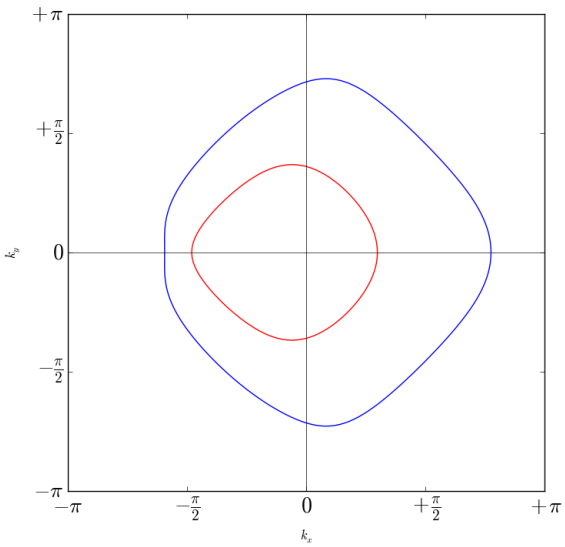

(a) Small in-plane field

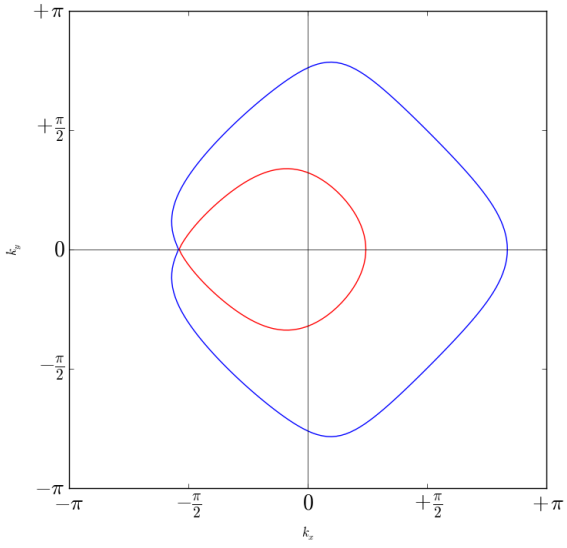

(b) In-plane field of equal magnitude to SOC

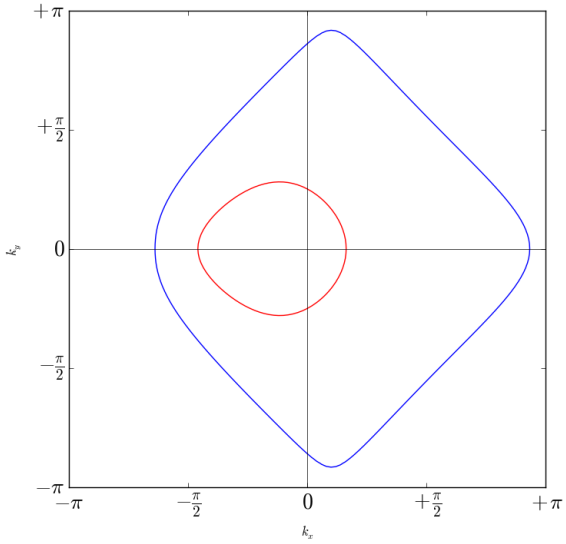

(c) Large in-plane field

Figure 3: Shown are Fermi surfaces for the system with an added in-plane magnetic field, in the y-direction. The two bands are notably displaced from the center, but are also importantly not centro-symmetric. In 3b we see that the Fermi surfaces touch, this happens for equal strength SOC and B-field. [1]

$$H_B = \sum_{i,s,s'} \frac{1}{2}[H_x(\sigma_x)_{ss'} + H_y(\sigma_y)_{ss'}]c^\dagger_{i,s}c_{i,s'} \tag{34}$$

Inserting the Pauli spin matrices and going to momentum space:

$$H_B = \sum_{i,s} \frac{1}{2}[H_x - isH_y]c^\dagger_{i,s}c_{i,-s}$$
$$= \sum_{\boldsymbol{k},s} \frac{1}{2}[H_x - isH_y]c^\dagger_{\boldsymbol{k},s}c_{\boldsymbol{k},-s} \tag{35}$$

This Hamiltonian has the same structure as (20) which means that by redefining $A_{\boldsymbol{k}}$ as

$$A_{\boldsymbol{k}} = A(\sin(k_y) + i\sin(k_x)) + H_x - iH_y \tag{36}$$

and as a result, Φ_k to

$$\Phi_{\boldsymbol{k}} = \frac{A[\sin(k_y) + i\sin(k_x)] + H_x - iH_y}{|A[\sin(k_y) + i\sin(k_x)] + H_x - iH_y|} \tag{37}$$

the results from the previous section remain unchanged, and the transformations in (31) are the same.

To compare with [34] we set $H_y = 0$, $H_x \gg A$, and then expand $\Phi_{\boldsymbol{k}}$. In this large in-plane field limit, $\Phi_{\boldsymbol{k}}$ is almost real, and so we write

$$e^{i\gamma_{\boldsymbol{k}}} = \Phi_{\boldsymbol{k}} \tag{38}$$

From the definition of $\Phi_{\boldsymbol{k}}$ in (37), we have

$$\tan(\gamma_{\boldsymbol{k}}) = \frac{A}{H_x}\left(\frac{\sin(k_x)}{\frac{A}{H_x}\sin(k_y) + 1}\right) \tag{39}$$

We expand $e^{ix} = 1 + ix - \frac{x^2}{2} + \mathcal{O}(x^3)$, $\arctan(x) = x + \mathcal{O}(x^3)$ and $\frac{1}{1+x} = 1 - x + \mathcal{O}(x^2)$. Since the in-plane field is very large, we only keep terms of $\mathcal{O}\left(\frac{A^2}{H_x^2}\right)$. Hence

$$e^{i\gamma_{\boldsymbol{k}}} \sim 1 - i\frac{A}{H_x}\sin(k_x) + \frac{A^2}{H_x^2}\sin(k_x)(i\sin(k_y) - \frac{1}{2}\sin(k_x)). \tag{40}$$

Below we will end up with a potential that goes as $\Phi_{\boldsymbol{k}}\Phi^\dagger_{\boldsymbol{k}'}$, and when using the above expansion the potential reads

$$\Phi_{\boldsymbol{k}}\Phi^\dagger_{\boldsymbol{k}'} \sim 1 + \frac{A}{H_x}(\sin(k'_x) - \sin(k_x)) - \frac{A^2}{H_x^2}\left(\frac{1}{2}(\sin(k'_x) - \sin(k_x))^2 + i(\sin(k'_x)\sin(k'_y) - \sin(k_x)\sin(k_y))\right). \tag{41}$$

Note that the imaginary term does not break hermiticity because there is in the Hamiltonian a sum over both k and k'. Therefore only the sum $\Gamma_{\alpha,\alpha'}\Phi_{\boldsymbol{k}}\Phi^\dagger_{\boldsymbol{k}'}\ a^\dagger_{\boldsymbol{k},\alpha}a^\dagger_{-\boldsymbol{k}+\boldsymbol{q},\beta}a_{-\boldsymbol{k}'+\boldsymbol{q},\beta'}a_{\boldsymbol{k}',\alpha'} + \Gamma_{\alpha',\alpha}\Phi_{\boldsymbol{k}'}\Phi^\dagger_{\boldsymbol{k}}\ a^\dagger_{\boldsymbol{k}',\alpha'}a^\dagger_{-\boldsymbol{k}'+\boldsymbol{q},\beta'}a_{-\boldsymbol{k}+\boldsymbol{q},\beta}a_{\boldsymbol{k},\alpha}$ needs to be hermitian, or in other words the potential must remain unchanged under the simultaneous operations of hermitian conjugate, $\alpha, \beta, \beta', \alpha' \to \alpha', \beta', \beta, \alpha$ and $\boldsymbol{k}, \boldsymbol{k}' \to \boldsymbol{k}', \boldsymbol{k}$.

Next is a comparison between the transformations (32) in this high in-plane field limit, and the corresponding transformations used in [34] which read

$$(c_{\boldsymbol{k},\uparrow})_x = \left[1 - \frac{k_x^2A^2}{8H_x^2}\right]a_{\boldsymbol{k},1} - i\frac{k_xA}{2H_x}a_{\boldsymbol{k},2}$$
$$(c_{\boldsymbol{k},\downarrow})_x = \left[1 - \frac{k_x^2A^2}{8H_x^2}\right]a_{\boldsymbol{k},2} - i\frac{k_xA}{2H_x}a_{\boldsymbol{k},1} \tag{42}$$

where we have used the notation in this text, and set the magnetic field to be entirely in-plane. To compare with these transformations, note that the transformations (32) can be multiplied by an arbitrary complex phase without changing the Hamiltonian. To get the same structure as Starykh et al. we multiply on the right side by the phase $e^{\frac{\gamma_{\boldsymbol{k}}}{2}}$. For an in-plane only field, they have also quantized the spin along the x-axis, and so a spin rotation $e^{i\frac{\pi}{4}\sigma_y}$ by $-90°$ is also included.

$$\begin{aligned}\begin{pmatrix} c_{\boldsymbol{k},\uparrow} \\ c_{\boldsymbol{k},\downarrow} \end{pmatrix}_x &= \frac{1}{\sqrt{2}} \begin{pmatrix} 1 & 1 \\ -1 & 1 \end{pmatrix} \begin{pmatrix} c_{\boldsymbol{k},\uparrow} \\ c_{\boldsymbol{k},\downarrow} \end{pmatrix}_z \\ &= \begin{pmatrix} \mathrm{Re}(e^{\frac{i}{2}\gamma_{\boldsymbol{k}}})a_{\boldsymbol{k},1} + i\mathrm{Im}(e^{\frac{i}{2}\gamma_{\boldsymbol{k}}})a_{\boldsymbol{k},2} \\ -i\mathrm{Im}(e^{\frac{i}{2}\gamma_{\boldsymbol{k}}})a_{\boldsymbol{k},1} - \mathrm{Re}(e^{\frac{i}{2}\gamma_{\boldsymbol{k}}})a_{\boldsymbol{k},2} \end{pmatrix} \\ &= \begin{pmatrix} \left[1 - \frac{A^2}{8H_x^2}\sin^2(k_x)\right] a_{\boldsymbol{k},1} + i\left[\frac{A}{2H_x}\sin(k_x) - \frac{A^2}{2H_x^2}\sin(k_x)\sin(k_y)\right] a_{\boldsymbol{k},2} \\ -\left[1 - \frac{A^2}{8H_x^2}\sin^2(k_x)\right] a_{\boldsymbol{k},2} - i\left[\frac{A}{2H_x}\sin(k_x) - \frac{A^2}{2H_x^2}\sin(k_x)\sin(k_y)\right] a_{\boldsymbol{k},1} \end{pmatrix}\end{aligned} \tag{43}$$

In the continuum limit which is what Starykh et al. were working on, $(\sin(k_x), \sin(k_y)) \to (k_x, k_y)$. Even so, there is an extra term $i\frac{A^2}{2H_x^2}\sin(k_x)\sin(k_y)$ that is not present in (42), and also the signs of the terms proportional to $a_{\boldsymbol{k},2}$ are different. Unfortunately the cause of this is unknown. The terms are to the same order $\mathcal{O}\left(\frac{A^2}{H_x^2}\right)$ as [34], though there is a difference in terms of rotational symmetry which is absent in this square lattice while present in the continuum case. Investigating this difference would be of interest for further work.

III. BCS MODEL

The fundamental interaction of BCS theory is an attractive potential that affects fermions in a small shell around the Fermi level [2]. This interaction could for example be electron-phonon-electron interactions [35]. In this thesis we are working however with a purely phenomenological potential, and so the origin of this BCS potential is of little interest. We assume that there is such a potential, and do not speculate on the cause.

A general spin-space BCS interaction can be written in momentum space as

$$H_{BCS} = \sum_{\boldsymbol{k},\boldsymbol{k'},\boldsymbol{q}} \sum_{s,s'} V_{s,s'}(\boldsymbol{k},\boldsymbol{k'}) c^\dagger_{\boldsymbol{k}+\boldsymbol{q},s} c^\dagger_{\boldsymbol{k'}-\boldsymbol{q},s'} c_{\boldsymbol{k'},s'} c_{\boldsymbol{k},s}, \tag{44}$$

where the potential scatters two fermions with momenta and spin $\boldsymbol{k}, s$ and $\boldsymbol{k'}, s'$ into two fermions with other momenta but the same spins $\boldsymbol{k}+\boldsymbol{q}, s$ and $\boldsymbol{k'}-\boldsymbol{q}, s'$. These momenta are assumed as mentioned above to all be in a small shell around the Fermi level. For a simple model with only kinetic energy terms, the Fermi surfaces will look similar to the one shown in Figure 1a. On this kind of centrosymmetric surface, there is a configuration which has as a property that for all $\boldsymbol{k}, \boldsymbol{q}$ such that $\boldsymbol{k}, \boldsymbol{k}+\boldsymbol{q}$ are in the shell, $\boldsymbol{k'}, \boldsymbol{k'}-\boldsymbol{q}$ must also be in the shell. It is simply $\boldsymbol{k'} = -\boldsymbol{k}$, while in all other configurations there are $\boldsymbol{k}, \boldsymbol{q}$ that do not fulfil the requirement of being in the shell. Thus we expect the dominant contribution to come from this particular configuration, since it has the largest available phase space. With this in mind we rewrite: $\boldsymbol{q} \to \boldsymbol{k} - \boldsymbol{k'}$, $\boldsymbol{k} \to \boldsymbol{k'}$, $\boldsymbol{k'} \to -\boldsymbol{k'} + \boldsymbol{q}$. This $\boldsymbol{q}$ is the offset from the dominant $\boldsymbol{k}, -\boldsymbol{k}$ contribution, or in other words the center of mass momentum (COMM) of the pair. An example of a single band interaction like this is shown in figure 4a, where it is clear that $\boldsymbol{q} = 0$ maximizes the available phase space. In the new notation equation (44) reads:

$$H_{BCS} = \sum_{\boldsymbol{k},\boldsymbol{k'},\boldsymbol{q}} \sum_{s,s'} V_{s,s'}(\boldsymbol{k},\boldsymbol{k'}) c^\dagger_{\boldsymbol{k},s} c^\dagger_{-\boldsymbol{k}+\boldsymbol{q},s'} c_{-\boldsymbol{k'}+\boldsymbol{q},s'} c_{\boldsymbol{k'},s} \tag{45}$$

When SOC interaction is added to the problem and the bands split, other types of BCS interaction can be included, namely interband and pair hopping interactions. This is determined by the band indices in the field operators. Interband interactions would go as $a^\dagger_{\boldsymbol{k},\alpha} a^\dagger_{-\boldsymbol{k}+\boldsymbol{q},\beta} a_{-\boldsymbol{k'}+\boldsymbol{q},\beta} a_{-\boldsymbol{k},\alpha}$ while pair hopping terms as $a^\dagger_{\boldsymbol{k},\alpha} a^\dagger_{-\boldsymbol{k}+\boldsymbol{q},\alpha} a_{-\boldsymbol{k'}+\boldsymbol{q},\beta} a_{-\boldsymbol{k},\beta}$. In this way, pair hopping terms are interactions that move pairs from one band to the other, while interband terms involve pairs that are on opposite bands. As can be seen in Figure 1, the SOC split keeps the surfaces concentric and

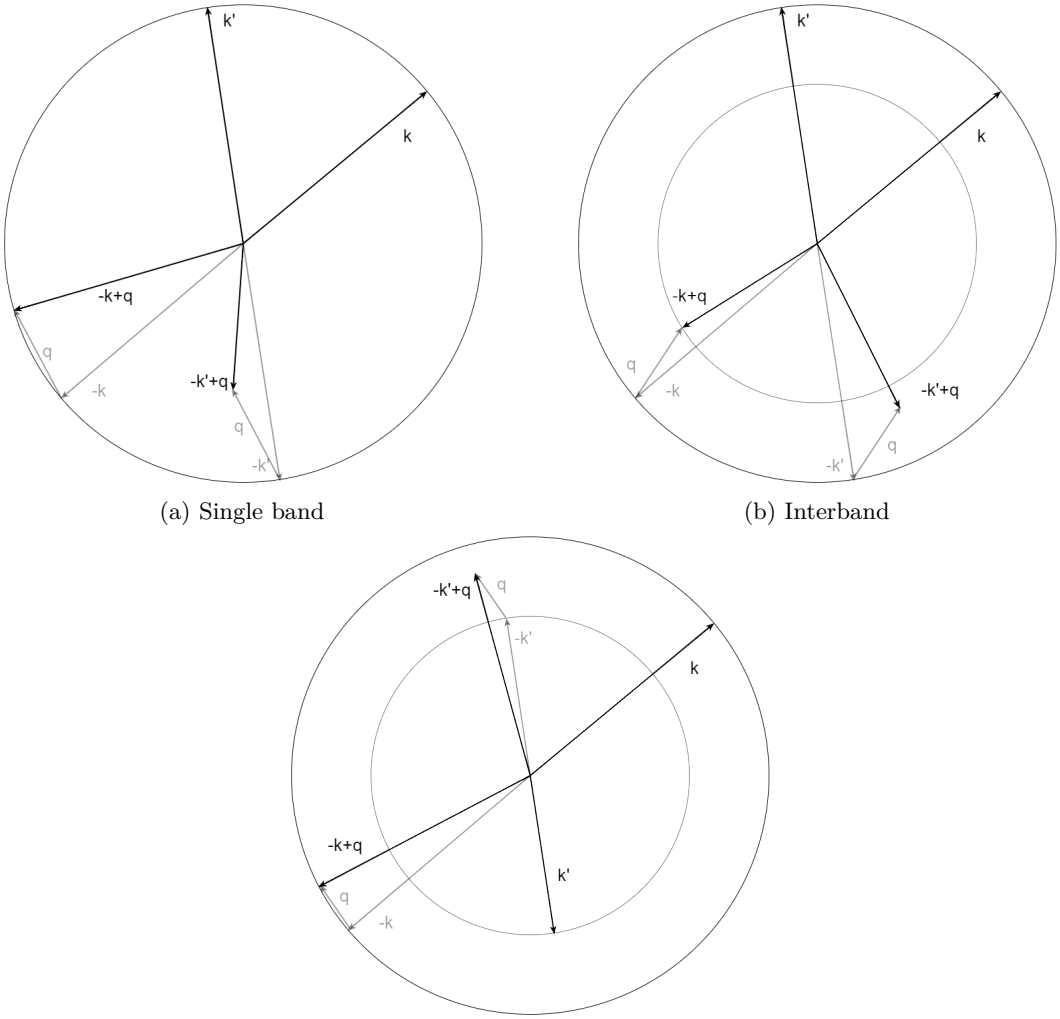

(a) Single band

(b) Interband

(c) Pair hopping

Figure 4: Shown are three types of pairing. 4a shows single band or intraband pairing, 4b shows interband pairing and 4c shows pair hopping. Shown are examples of concentric Fermi surfaces, for instance the two bands in our SOC split model. The vectors k, k', q correspond to pair hopping (a) and $\alpha\beta\beta\alpha$-type interband (b).

centrosymmetric, which means that the intraband terms as in the one band case have dominant contributions from $\boldsymbol{q} = 0$. This is also true for the pair hopping interaction shown in 4c. However, in Figure 4b it is clear that interband interactions do not have contributions at all from $\boldsymbol{q} = 0$, and require in general a momentum dependent $\boldsymbol{q} = \boldsymbol{q}(\boldsymbol{k}, \boldsymbol{k'})$ to maximize phase space. If one also includes an in-plane magnetic field, the Fermi surfaces will look like Figure 3 and these surfaces are deformed and displaced, and so in this case $\boldsymbol{q} = 0$ is not necessarily the dominant contribution even for intraband and pair hopping terms. We see the surfaces are displaced in opposite directions, and so picking out two COMMs as twice the center of each surface would function similarly to the SOC only case with respect to intraband pairing, with some inaccuracy from the deformations. This is what is done in [1], to optimize intraband pairing on each band.

A. Applying BCS to an SOC split model

We are ready to apply the BCS interaction, with the purpose of finding requirements for having chiral p-wave gaps, of the form $\Delta_{\boldsymbol{k}} \sim k_x + ik_y$.

A general BCS type interaction in the helicity basis can be written as:

$$H_I = \sum_{\boldsymbol{k},\boldsymbol{k'},\boldsymbol{q}} \sum_{\alpha,\alpha',\beta,\beta'} V_{\alpha,\alpha',\beta,\beta'}(\boldsymbol{k},\boldsymbol{k'},\boldsymbol{q}) a^\dagger_{k,\alpha} a^\dagger_{-k+q,\beta} a_{-k'+q,\beta'} a_{k',\alpha'}, \tag{46}$$

To preserve hermiticity we require $V^\dagger_{\alpha,\alpha',\beta,\beta'}(\boldsymbol{k},\boldsymbol{k'},\boldsymbol{q}) = V_{\alpha',\alpha,\beta',\beta}(\boldsymbol{k},\boldsymbol{k'},\boldsymbol{q})$. Using the transformations in equation (31), we return to the spin basis version of this interaction. Inserting directly yields:

$$\begin{aligned} H_I = \sum_{\boldsymbol{k},\boldsymbol{k'},\boldsymbol{q}} \sum_{\alpha,\alpha',\beta,\beta'} \frac{V_{\alpha,\alpha',\beta,\beta'}(\boldsymbol{k},\boldsymbol{k'},\boldsymbol{q})}{4} (c_{\boldsymbol{k},\uparrow} + \Gamma_{1\alpha}\Phi_{\boldsymbol{k}} c_{\boldsymbol{k},\downarrow})(c_{-\boldsymbol{k}+\boldsymbol{q},\uparrow} + \Gamma_{1\beta}\Phi_{-\boldsymbol{k}+\boldsymbol{q}} c_{-\boldsymbol{k}+\boldsymbol{q},\downarrow}) \\ \cdot (c_{-\boldsymbol{k'}+\boldsymbol{q},\uparrow} + \Gamma_{1\beta'}\Phi_{-\boldsymbol{k'}+\boldsymbol{q}} c_{-\boldsymbol{k'}+\boldsymbol{q},\downarrow})(c_{\boldsymbol{k'},\uparrow} + \Gamma_{1\alpha'}\Phi_{\boldsymbol{k'}} c_{\boldsymbol{k'},\downarrow}). \end{aligned} \tag{47}$$

In this equation, every one of the 16 combinations of spins are present, so by introducing new functions

$$Z_{s\alpha}(\boldsymbol{k}) \begin{cases} 1 & \text{if } s = \uparrow \\ \Gamma_{1\alpha}\Phi_{\boldsymbol{k}} & \text{if } s = \downarrow \end{cases} \tag{48}$$

we can rewrite equation (47) as

$$H_I = \sum_{\boldsymbol{k},\boldsymbol{k'},\boldsymbol{q}} \sum_{\alpha,\alpha',\beta,\beta'} \sum_{s,s',\sigma,\sigma'} \frac{V_{\alpha,\alpha',\beta,\beta'}(\boldsymbol{k},\boldsymbol{k'},\boldsymbol{q})}{4} Z^\dagger_{s\alpha}(\boldsymbol{k}) Z^\dagger_{\sigma\beta}(-\boldsymbol{k}+\boldsymbol{q}) Z_{\sigma'\beta'}(-\boldsymbol{k'}+\boldsymbol{q}) Z_{s'\alpha'}(\boldsymbol{k'}) c^\dagger_{\boldsymbol{k},s} c^\dagger_{-\boldsymbol{k}+\boldsymbol{q},\sigma} c_{-\boldsymbol{k'}+\boldsymbol{q},\sigma'} c_{\boldsymbol{k'},s'}. \tag{49}$$

This is an equation that determines what the potential is in the spin basis, when given a potential in the helicity basis. It is of interest, since one generally looks at interactions that have their origin in ordinary Fermions with spin rather than the quasiparticle excitations in a given model. Since the potential is arbitrary, we try to find one that is as simple as possible and thus solvable, in both the helicity and spin bases, while giving a chiral p-wave gap function.

We pick out a potential that has only two indices in the following manner:

$$V_{\alpha,\alpha',\beta,\beta'}(\boldsymbol{k},\boldsymbol{k'},\boldsymbol{q}) \propto \delta_{\alpha\beta}\delta_{\alpha'\beta'}. \tag{50}$$

Inserting this into equation (46), the coupling becomes as $a^\dagger_{\boldsymbol{k},\alpha} a^\dagger_{-\boldsymbol{k}+\boldsymbol{q},\alpha} a_{-\boldsymbol{k'}+\boldsymbol{q},\alpha'} a_{\boldsymbol{k'},\alpha'}$. This choice of potential is convenient, because the coupling then describes both intraband pairing and pair hopping, for $\alpha = \alpha'$ and $\alpha \neq \alpha'$, respectively. As described previously, the choice of $\boldsymbol{q} = 0$ will maximize the phase space for these interactions, and as such be the dominant contribution. As for interband interactions, since $\boldsymbol{k}$ and $-\boldsymbol{k} + \boldsymbol{q}$ have to be on opposite bands in this case and the bands are centrosymmetric, there is no one $\boldsymbol{q}$ that can satisfy this for all $\boldsymbol{k}$. For the case of Figure 4b, there are two $\boldsymbol{q}$-values that satisfy our requirement, the intersections between two displaced copies of the inner band. In general this isn't necessarily the case, if the band split is large enough there will be for certain momenta $\boldsymbol{k}, \boldsymbol{k'}$ no intersections and thus no $\boldsymbol{q}$-values that satisfy our requirement. However even for the cases that do have $\boldsymbol{q}$-values that are satisfactory, they must be dependent on the other momenta $\boldsymbol{k}, \boldsymbol{k'}$ and the shape of the surface itself in a nontrivial way. To avoid this we therefore choose a potential that sidesteps this problem by only including intraband and pairhopping terms. In the following, we will drop the sum over $\boldsymbol{q}$ and use (19), that is no in-plane magnetic field.

To proceed one should diagonalize the total Hamiltonian given as the sum of (46) and (24) to find the eigenstates and energy spectrum of the system. However, this is difficult, so an approximation is required. We use a Mean-Field approximation to reduce the interaction to a one-particle problem, and define

$$b_{\alpha\alpha'}(\boldsymbol{k}) = < a_{-\boldsymbol{k},\alpha} a_{\boldsymbol{k},\alpha'} > . \tag{51}$$

$b_{\alpha\alpha'}(\boldsymbol{k})$ is the expectation value of this particular combination of field operators. The approximation is to assume that the field operators deviate only slightly around this expectation value, and we write

$$a_{-\boldsymbol{k},\alpha}a_{\boldsymbol{k},\alpha'} = b_{\alpha\alpha'}(\boldsymbol{k}) + (a_{-\boldsymbol{k},\alpha}a_{\boldsymbol{k},\alpha'} - b_{\alpha\alpha'}(\boldsymbol{k})) = b_{\alpha\alpha'}(\boldsymbol{k}) + \delta_{\alpha\alpha'}(\boldsymbol{k}) \tag{52}$$

with $\delta_{\alpha\alpha'}(\boldsymbol{k})$ as the deviation. Since it is assumed small, we ignore all terms of $\mathcal{O}(\delta_{\alpha\alpha'}(\boldsymbol{k})^2)$. Rewriting the interaction Hamiltonian (46) using equation (52), and ignoring higher powers of $\delta_{\alpha\alpha'}(\boldsymbol{k})$, we get the result

$$H_I = \sum_{\boldsymbol{k},\boldsymbol{k'}}\sum_{\alpha,\alpha'} V_{\alpha,\alpha'}(\boldsymbol{k},\boldsymbol{k'},\boldsymbol{q})[b^\dagger_{\alpha\alpha}(\boldsymbol{k})a_{-\boldsymbol{k'},\alpha'}a_{\boldsymbol{k'},\alpha'} + b_{\alpha'\alpha'}(\boldsymbol{k'},\boldsymbol{q})a^\dagger_{\boldsymbol{k},\alpha}a^\dagger_{-\boldsymbol{k},\alpha} - b^\dagger_{\alpha\alpha}(\boldsymbol{k})b_{\alpha'\alpha'}(\boldsymbol{k'},\boldsymbol{q})]. \tag{53}$$

This Hamiltonian is much simpler, being bilinear the field operators. Thus we can diagonalize the total Hamiltonian in order to find the gap equations. We introduce the order parameters

$$\Delta_\alpha(\boldsymbol{k}) = \sum_{\boldsymbol{k'},\alpha'} V_{\alpha,\alpha'}(\boldsymbol{k},\boldsymbol{k'},\boldsymbol{q})b_{\alpha'\alpha'}(\boldsymbol{k'},\boldsymbol{q}). \tag{54}$$

and rewrite equation (53) as

$$H_I = \sum_{\boldsymbol{k},\alpha} \Delta_\alpha(\boldsymbol{k})a^\dagger_{\boldsymbol{k},\alpha}a^\dagger_{-\boldsymbol{k},\alpha} + \Delta^\dagger_\alpha(\boldsymbol{k})a_{-\boldsymbol{k},\alpha}a_{\boldsymbol{k},\alpha} + \Delta_\alpha(\boldsymbol{k})b^\dagger_{\alpha\alpha}(\boldsymbol{k}) \tag{55}$$

Including the entire Hamiltonian, meaning the sum of equations (55) and (24), omitting constant terms, and rewriting to matrix form gives:

$$H = \sum_{\boldsymbol{k}} \xi^\dagger_{\boldsymbol{k}} \begin{bmatrix} \frac{E_{1,\boldsymbol{k}}}{2} & \Delta^\dagger_1(\boldsymbol{k}) & 0 & 0 \\ \Delta_1(\boldsymbol{k}) & \frac{-E_{1,-\boldsymbol{k}}}{2} & 0 & 0 \\ 0 & 0 & \frac{E_{2,\boldsymbol{k}}}{2} & \Delta^\dagger_2(\boldsymbol{k}) \\ 0 & 0 & \Delta_2(\boldsymbol{k}) & \frac{-E_{2,-\boldsymbol{k}}}{2} \end{bmatrix} \xi_{\boldsymbol{k}}, \tag{56}$$

for

$$\xi^\dagger_{\boldsymbol{k}} = (a^\dagger_{\boldsymbol{k},1} \;\; a_{-\boldsymbol{k},1} \;\; a^\dagger_{\boldsymbol{k},2} \;\; a_{-\boldsymbol{k},2}). \tag{57}$$

This matrix is easily diagonalizable being block diagonal, and the eigenvalues are:

$$\lambda^\pm_\alpha(\boldsymbol{k}) = \frac{E_{\alpha,\boldsymbol{k}} - E_{\alpha,-\boldsymbol{k}}}{4} \pm \sqrt{\left(\frac{E_{\alpha,\boldsymbol{k}} + E_{\alpha,-\boldsymbol{k}}}{4}\right)^2 + |\Delta_\alpha(\boldsymbol{k})|^2}. \tag{58}$$

Since $A_{\boldsymbol{k}} = -A_{-\boldsymbol{k}}$ and $\epsilon_{-\boldsymbol{k}} = \epsilon_{\boldsymbol{k}}$, the energy $E_{\alpha,\boldsymbol{k}}$ is symmetric in $\boldsymbol{k}$, so that inserting equation (23) yields

$$\lambda^\pm_\alpha(\boldsymbol{k}) = \pm\sqrt{\left(\frac{\epsilon_{\boldsymbol{k}} + \Gamma_{1\alpha}|A_{\boldsymbol{k}}| - \mu}{2}\right)^2 + |\Delta_\alpha(\boldsymbol{k})|^2}. \tag{59}$$

Equation (59) is the energy value of the new Fermi operators $\eta_{\boldsymbol{k},\alpha}, \gamma_{\boldsymbol{k}\alpha}$, defining the basis in which the total Hamiltonian is diagonal,

$$H = \sum_{\boldsymbol{k},\alpha} \lambda_\alpha(\boldsymbol{k})(\eta_{\boldsymbol{k},\alpha} - \gamma_{\boldsymbol{k}\alpha}) + H_0 \tag{60}$$

where we have defined $\lambda_\alpha(\boldsymbol{k}) = \lambda^+_\alpha(\boldsymbol{k})$ and $H_0 = -\Delta_\alpha(\boldsymbol{k})b^\dagger_{\alpha\alpha}(\boldsymbol{k})$.
Since this is of the form of a free Fermi gas, we can use the partition function

$$Z = \prod_{\boldsymbol{k},\alpha} (1 + e^{-\beta\lambda_\alpha(\boldsymbol{k})})(1 + e^{\beta\lambda_\alpha(\boldsymbol{k})})e^{-\beta H_0}, \tag{61}$$

with $\beta = \frac{1}{k_B T}$ where k_B is Boltzmann's constant and T is temperature, along with the free energy

$$F = -\frac{1}{\beta}\log(Z) \tag{62}$$

to determine the gap functions $\Delta_\alpha(\boldsymbol{k})$. To do this, we differentiate the free energy with respect to the gap function to minimize it, and use that in thermodynamic equilibrium the system will come to rest in a state that minimizes the free energy:

$$\begin{aligned}
\frac{\partial F}{\partial \Delta_{\alpha'}(\boldsymbol{k}')} &= -\frac{1}{\beta}\frac{\partial}{\partial \Delta_{\alpha'}(\boldsymbol{k}')}\sum_{\boldsymbol{k},\alpha}\left(\log(1 + e^{-\beta\lambda_\alpha(\boldsymbol{k})}) + \log(1 + e^{\beta\lambda_\alpha(\boldsymbol{k})}) + \log e^{-\beta H_0}\right) \\
&= \frac{\partial \lambda_{\alpha'}(\boldsymbol{k}')}{\partial \Delta_{\alpha'}(\boldsymbol{k}')}\left(\frac{e^{-\beta\lambda_{\alpha'}(\boldsymbol{k}')}}{1 + e^{-\beta\lambda_{\alpha'}(\boldsymbol{k}')}} - \frac{e^{\beta\lambda_{\alpha'}(\boldsymbol{k}')}}{1 + e^{\beta\lambda_{\alpha'}(\boldsymbol{k}')}}\right) + \frac{\partial H_0}{\partial \Delta_{\alpha'}(\boldsymbol{k}')} \\
&= \frac{\partial \lambda_{\alpha'}(\boldsymbol{k}')}{\partial \Delta_{\alpha'}(\boldsymbol{k}')}\tanh\left(\frac{-\beta\lambda_{\alpha'}(\boldsymbol{k}')}{2}\right) + \frac{\partial H_0}{\partial \Delta_{\alpha'}(\boldsymbol{k}')}.
\end{aligned} \tag{63}$$

The two derivatives are

$$\frac{\partial \lambda_{\alpha'}(\boldsymbol{k}')}{\partial \Delta_{\alpha'}(\boldsymbol{k}')} = \frac{\Delta^\dagger_{\alpha'}(\boldsymbol{k}')}{2\lambda_{\alpha'}(\boldsymbol{k}')} \tag{64}$$

$$\frac{\partial H_0}{\partial \Delta_{\alpha'}(\boldsymbol{k}')} = -b^\dagger_{\alpha'\alpha'}(\boldsymbol{k}') \tag{65}$$

treating $\Delta_{\alpha'}(\boldsymbol{k}')$ and $\Delta^\dagger_{\alpha'}(\boldsymbol{k}')$ as different variables. Setting equation (63) equal to zero, inserting the derivatives, multiplying both sides with $V_{\alpha,\alpha'}(\boldsymbol{k},\boldsymbol{k}')$, and summing over $\alpha', \boldsymbol{k}'$ yields

$$\Delta^\dagger_\alpha(k) = \sum_{k',\alpha'}\frac{\Delta^\dagger_{\alpha'}(k')}{2\lambda_{\alpha'}(k')}\tanh\left(\frac{-\beta\lambda_{\alpha'}(k')}{2}\right)V_{\alpha,\alpha'}(k,k'), \tag{66}$$

where we have used the hermitian conjugate of equation (54) to obtain $\Delta^\dagger_\alpha(k)$. There is another gap equation for $\Delta_\alpha(\boldsymbol{k})$, the hermitian conjugate of equation (66), which is obtainable by differentiating with respect to $\Delta^\dagger_\alpha(\boldsymbol{k})$ instead of $\Delta_\alpha(\boldsymbol{k})$. It is possible to solve these gap equations self consistently using numerical methods. However it is important to note that in setting equation (63) to zero we have merely obtained an extremum. Unless multiple solutions exist this must be a minimum since the free energy must be bound from below, but in the event of multiple solutions one must insert the gap functions back into the free energy to confirm which is the proper minimum. In this case, the specific numerics are of little interest and so we assume that we pick out the correct solution in the following.

We are interested in what potential inserted into this equation will yield a chiral p-wave gap function. A simple separable potential is convenient, so we set

$$V_{\alpha\alpha'}(\boldsymbol{k},\boldsymbol{k}') = VU^\dagger_\alpha(\boldsymbol{k})U_{\alpha'}(\boldsymbol{k}')v_{\alpha,\alpha'}, \tag{67}$$

where V is a constant, $U_\alpha(\boldsymbol{k})$ and $v_{\alpha,\alpha'}$ can be any functions at this point, with the restriction that $V_{\alpha\alpha'}(\boldsymbol{k},\boldsymbol{k}') = V^\dagger_{\alpha'\alpha}(\boldsymbol{k}',\boldsymbol{k})$. Below we insert $U_\alpha(\boldsymbol{k}) = A_{\boldsymbol{k}}$, $v_{\alpha,\alpha'} = \Gamma_{\alpha,\alpha'}$, as it leads to a chiral p-wave gap, and a simple expression in spin-space when inserted into equation (49). Inserting the potential (67) into equation (66) gives

$$\Delta_\alpha^\dagger(\boldsymbol{k}) = \left(\sum_{\boldsymbol{k}',\alpha'} \Delta_{\alpha'}^\dagger(\boldsymbol{k}')\chi_{\alpha'}(\boldsymbol{k}')v_{\alpha,\alpha'}U_{\alpha'}(\boldsymbol{k}') \right) U_\alpha^\dagger(\boldsymbol{k}), \tag{68}$$

with $\chi_{\alpha'}(\boldsymbol{k}') = \frac{1}{2\lambda_{\alpha'}(\boldsymbol{k}')} \tanh\left(\frac{-\beta\lambda_{\alpha'}(\boldsymbol{k}')}{2}\right)$. Equation (68) determines the $\boldsymbol{k}$-dependence of $\Delta_\alpha(\boldsymbol{k})$ as

$$\Delta_\alpha^\dagger(\boldsymbol{k}) = \Delta_\alpha^\dagger U_\alpha^\dagger(\boldsymbol{k}), \tag{69}$$

defining $\Delta_\alpha^\dagger = \left(\sum_{\boldsymbol{k}',\alpha'} \Delta_{\alpha'}^\dagger(\boldsymbol{k}')\chi_{\alpha'}(\boldsymbol{k}')v_{\alpha,\alpha'}U_{\alpha'}(\boldsymbol{k}') \right)$. Choosing $U_\alpha(\boldsymbol{k}) = A_{\boldsymbol{k}}^\dagger$ we see

$$\Delta_\alpha(\boldsymbol{k}) = A\Delta_\alpha(\sin(k_y) + i\sin(k_x)), \tag{70}$$

which is exactly a chiral p-wave gap function. Of course, using a different function $U_\alpha(\boldsymbol{k})$ can yield any $\boldsymbol{k}$-dependence as desired. It is important to stress that this is assuming a potential that both leads to zero interband interaction terms and also is separable. In principle, an equation similar to (68) with a non-separable potential could be used, but to find the $\boldsymbol{k}$-dependence would involve numerical self consistent solutions.

We have at this point a chiral p-wave gap, and so we wish to know what kind of spin space interaction would cause this. Returning to the potential in (67), and inserting this potential into equation (49) to discover the spin space representation of this interaction yields

$$H_I = V \sum_{\boldsymbol{k},\boldsymbol{k}'} \sum_{\alpha,\alpha'} \sum_{s,s',\sigma,\sigma'} \frac{A_{\boldsymbol{k}} A_{\boldsymbol{k}'}^\dagger \Gamma_{\alpha\alpha'}}{4} Z_{s\alpha}^\dagger(\boldsymbol{k}) Z_{\sigma\alpha}^\dagger(-\boldsymbol{k}) Z_{\sigma'\alpha'}(-\boldsymbol{k}') Z_{s'\alpha'}(\boldsymbol{k}') c_{\boldsymbol{k},s}^\dagger c_{-\boldsymbol{k},\sigma}^\dagger c_{-\boldsymbol{k}',\sigma'} c_{\boldsymbol{k}',s'}. \tag{71}$$

$\Gamma_{\alpha\alpha'}$ is antisymmetric in both α and α', and as a result of the sum over band indices, all terms that have an overall antisymmetric factor in either α or α' will vanish. The remaining terms will therefore, considering the definition of $Z_{s\alpha}$ from equation (48), have exactly one spin down from each of s, σ and s', σ' to cancel out the antisymmetry in the potential. In other words, $s = -\sigma$ and $s' = -\sigma'$, and we get the additional factors $\Gamma_{ss'}\Phi_{\boldsymbol{k}}^\dagger \Phi_{\boldsymbol{k}'}$:

$$H_I = V \sum_{\boldsymbol{k},\boldsymbol{k}'} \sum_{s,s',\sigma,\sigma'} \frac{A_{\boldsymbol{k}} A_{\boldsymbol{k}'}^\dagger}{4} \Gamma_{ss'} \Phi_k^\dagger \Phi_{\boldsymbol{k}'} c_{k,s}^\dagger c_{-k,-s}^\dagger c_{-k',-s'} c_{k',s'}. \tag{72}$$

As $\Phi_{\boldsymbol{k}}$ is the phase of $A_{\boldsymbol{k}}$, they cancel leaving only $|A_{\boldsymbol{k}}||A'_{\boldsymbol{k}}| = |A|^2\sqrt{(\sin^2(k_x) + \sin^2(k_y))(\sin^2(k'_x) + \sin^2(k'_y))}$. Performing also the sum over α, α' gives

$$H_I = V|A|^2 \sum_{\boldsymbol{k},\boldsymbol{k}'} \sum_{s,s'} \sqrt{(\sin^2(k_x) + \sin^2(k_y))(\sin^2(k'_x) + \sin^2(k'_y))} \Gamma_{ss'} c_{\boldsymbol{k},s}^\dagger c_{-\boldsymbol{k},-s}^\dagger c_{-\boldsymbol{k}',-s'} c_{\boldsymbol{k}',s'}, \tag{73}$$

which is the final spin space interaction for our particular chiral p-wave gap. In other words, this interaction, when transformed into helicity space will cause chiral p-wave gapped superconductivity. The continuum limit of this equation reads

$$H_I = V|A|^2 \sum_{\boldsymbol{k},\boldsymbol{k}'} \sum_{s,s'} |\boldsymbol{k}||\boldsymbol{k}'| \Gamma_{ss'} c_{\boldsymbol{k},s}^\dagger c_{-\boldsymbol{k},-s}^\dagger c_{-\boldsymbol{k}',-s'} c_{\boldsymbol{k}',s'}, \tag{74}$$

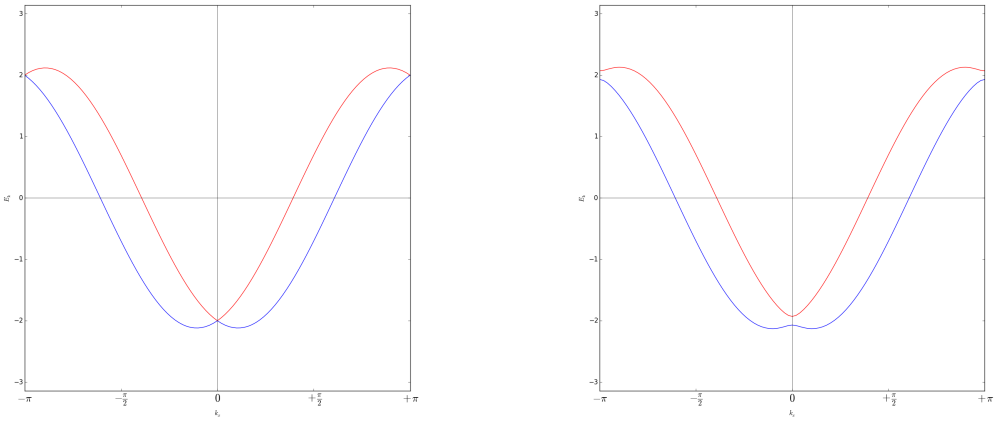

(a) Pair hopping

(b) Interband

Figure 5: X-plane slice of the Fermi levels, with only SOC and SOC and Zeeman B-field, respectively. The energy bands are separated by the B-field.

IV. OUT OF PLANE MAGNETIC FIELD

The Majorana edge states are of interest because they protect the superconductor as described above. However, each band will contribute one Majorana fermion each. A simple way to argue for this is to use the chemical potential [18]. Suppose that outside of the system is vacuum. Then there must be no states present outside the bulk. Hence the chemical potential is effectively negative and very large in this area. Then, at the boundary, the chemical potential should pass from the bulk value to the vacuum value. For convenience we shift the energy values $E_{\alpha,\boldsymbol{k}}$ so that $E_{2,0} = 0$, using the chemical potential. In other words, we set $\mu \to \mu' = \mu + E_{2,0}$. With this renaming of μ, if μ is positive in the bulk, it must be zero somewhere at the interface between bulk and vacuum. Keeping this in mind we look at the dispersion relation (59), for $(\mu, \boldsymbol{k}) \to (0, 0)$:

$$\lambda_\alpha^\pm(\boldsymbol{k}) = \pm\sqrt{\left(\frac{\Gamma_{1\alpha}|A|k - \mu}{2}\right)^2 + |A|^2|\Delta_\alpha|^2k^2}. \tag{75}$$

Here we have let $\epsilon_{\boldsymbol{k}} \to 0$ and $|A_{\boldsymbol{k}}| \to k$, as they should for sufficiently small k. Some reordering yields

$$\lambda_\alpha^\pm(\boldsymbol{k}) = \pm\sqrt{\mu^2\frac{|\Delta_\alpha|^2}{1+4|\Delta_\alpha|^2} + |A|^2\left(\frac{1}{4} + |\Delta_\alpha|^2\right)\left(k - \frac{\Gamma_{1\alpha}\mu}{|A|\,(1+4|\Delta_\alpha|^2)}\right)^2} \tag{76}$$

This shows that at the points on the interface for which $\mu = 0$ the states will be massless fermionic states with dispersion relation

$$\lambda_\alpha^\pm(\boldsymbol{k}) = \pm|A|\sqrt{\frac{1}{4} + |\Delta_\alpha|^2}\; k \tag{77}$$

If on the other hand μ is negative in the bulk, it never needs to pass through zero at the interface and this argument fails.

With only SOC we have $E_{1,0} = E_{2,0}$, and thus $\mu > 0$ means that both bands contribute. However there are ways of separating the bands to prevent this, allowing only one of the bands to contribute to the Majorana edge states. This is important because an odd number of edge state pairs become topologically trivial [7]. One way is to add a magnetic field $\boldsymbol{B}$ in the $\hat{z}$ direction, a Zeeman field. Figure 5 shows the energy values $E_{\alpha,\boldsymbol{k}}$ before BCS of our system without and with Zeeman field, respectively, for one particular k_y-value. As stated, the bands are separated by the Zeeman field. Next will be explicitly calculating the energy spectra of the Zeeman-shifted system, as well as checking how the

magnetic field affects equation (49), to establish conditions under which one can get a chiral p-wave superconductor protected by one-band surface Majorana fermions.

The $\boldsymbol{B}$-field will couple to the spins as

$$H_{\boldsymbol{B}} = \sum_i B\hat{z} \cdot \boldsymbol{S}_i \tag{78}$$

for $\boldsymbol{S_i} = \frac{\boldsymbol{\sigma}}{2} c^\dagger_{i,s} c_{i,s'}$, and after Fourier transforming into $\boldsymbol{k}$-space, and using the third Pauli matrix

$$\sigma_z = \begin{pmatrix} 1 & 0 \\ 0 & -1 \end{pmatrix}, \tag{79}$$

we have

$$H_{\boldsymbol{B}} = \sum_{\boldsymbol{k},s} B\Gamma_{1s} c^\dagger_{\boldsymbol{k},s} c_{\boldsymbol{k},s}. \tag{80}$$

Applying to this Hamiltonian the transformations in equation (32):

$$\begin{aligned} H_{\boldsymbol{B}} &= \sum_{\boldsymbol{k}} B\frac{1}{2}[(a^\dagger_{\boldsymbol{k},1} + a^\dagger_{\boldsymbol{k},2})(a_{\boldsymbol{k},1} + a_{\boldsymbol{k},2}) - \Phi_{\boldsymbol{k}}(a^\dagger_{\boldsymbol{k},1} - a^\dagger_{\boldsymbol{k},2})\Phi^\dagger_{\boldsymbol{k}}(a_{\boldsymbol{k},1} - a_{\boldsymbol{k},2})] \\ &= \sum_{\boldsymbol{k}} B(a^\dagger_{\boldsymbol{k},1} a_{\boldsymbol{k},2} + a^\dagger_{\boldsymbol{k},2} a_{\boldsymbol{k},1}). \end{aligned} \tag{81}$$

Adding this equation to equation (24) and rewriting into matrix form yields

$$H = \sum_{\boldsymbol{k}} \phi^\dagger_{\boldsymbol{k}} \begin{pmatrix} \epsilon_{\boldsymbol{k}} + |A_{\boldsymbol{k}}| & B \\ B & \epsilon_{\boldsymbol{k}} - |A_{\boldsymbol{k}}| \end{pmatrix} \phi_{\boldsymbol{k}}, \tag{82}$$

defining $\phi_{\boldsymbol{k}} = \begin{pmatrix} a_{\boldsymbol{k},1} \\ a_{\boldsymbol{k},2} \end{pmatrix}$. The eigenvalues of equation (82) are found to be

$$E^{B_z}_{\boldsymbol{k}} = \epsilon_{\boldsymbol{k}} \pm \sqrt{|A_{\boldsymbol{k}}|^2 + B^2}, \tag{83}$$

and as claimed these energy values are as the previous $E_{\boldsymbol{k}}$ SOC band spectra, but separated by the B-field.

Next it is of interest to see how the Zeeman field with affect equation (49). To find this we require the transformations from the SOC helicity basis into the SOC and Zeeman helicity basis. Since our matrix in equation (82) is not only hermitian but also real, we can find real orthogonal matrices to diagonalize it. We have

$$\begin{aligned} \begin{pmatrix} \epsilon_{\boldsymbol{k}} + \sqrt{|A_{\boldsymbol{k}}|^2 + B^2} & 0 \\ 0 & \epsilon_{\boldsymbol{k}} - \sqrt{|A_{\boldsymbol{k}}|^2 + B^2} \end{pmatrix} &= \begin{pmatrix} \cos(\theta_{\boldsymbol{k}}) & -\sin(\theta_{\boldsymbol{k}}) \\ \sin(\theta_{\boldsymbol{k}}) & \cos(\theta_{\boldsymbol{k}}) \end{pmatrix} \begin{pmatrix} \epsilon_{\boldsymbol{k}} + |A_{\boldsymbol{k}}| & B \\ B & \epsilon_{\boldsymbol{k}} - |A_{\boldsymbol{k}}| \end{pmatrix} \begin{pmatrix} \cos(\theta_{\boldsymbol{k}}) & \sin(\theta_{\boldsymbol{k}}) \\ -\sin(\theta_{\boldsymbol{k}}) & \cos(\theta_{\boldsymbol{k}}) \end{pmatrix} \\ &= \begin{pmatrix} \epsilon_{\boldsymbol{k}} + \cos(2\theta_{\boldsymbol{k}})|A_{\boldsymbol{k}}| - \sin(2\theta_{\boldsymbol{k}})B & \sin(2\theta_{\boldsymbol{k}})|A_{\boldsymbol{k}}| + \cos(2\theta_{\boldsymbol{k}})B \\ \sin(2\theta_{\boldsymbol{k}})|A_{\boldsymbol{k}}| + \cos(2\theta_{\boldsymbol{k}})B & \epsilon_{\boldsymbol{k}} + \cos(2\theta_{\boldsymbol{k}})|A_{\boldsymbol{k}}| + \sin(2\theta_{\boldsymbol{k}})B) \end{pmatrix}, \end{aligned} \tag{84}$$

which has as solution

$$\theta_{\boldsymbol{k}} = \frac{1}{2}\arctan\left(\frac{-B}{|A_{\boldsymbol{k}}|}\right). \tag{85}$$

The transformations are thus given as

$$\begin{pmatrix} \cos(\theta_{\boldsymbol{k}}) & \sin(\theta_{\boldsymbol{k}}) \\ -\sin(\theta_{\boldsymbol{k}}) & \cos(\theta_{\boldsymbol{k}}) \end{pmatrix} \begin{pmatrix} a_{\boldsymbol{k},1} \\ a_{\boldsymbol{k},2} \end{pmatrix} = \begin{pmatrix} d_{\boldsymbol{k},1} \\ d_{\boldsymbol{k},2} \end{pmatrix}$$

or

$$d_{\boldsymbol{k},\alpha} = \cos(\theta_{\boldsymbol{k}}) a_{\boldsymbol{k},\alpha} + \Gamma_{2\bar{\alpha}} \sin(\theta_{\boldsymbol{k}}) a_{\boldsymbol{k},\bar{\alpha}}, \tag{86}$$

with $d_{\boldsymbol{k},\alpha}$ as the SOC and Zeeman helicity band operators, and $\bar{\alpha}$ referring to the band index opposite of α. Constructing once again a general, intraband, BCS-type interaction in our new basis, we get exactly the same results as in equations (59) and (68), only now with $|A_{\boldsymbol{k}}| \to \sqrt{|A_{\boldsymbol{k}}|^2 + B^2}$ in the energy spectrum,

$$\lambda_{\alpha}^{\pm}(\boldsymbol{k}) = \pm \sqrt{\left(\frac{\epsilon_{\boldsymbol{k}} + \Gamma_{1\alpha}\sqrt{|A_{\boldsymbol{k}}|^2 + B^2} - \mu}{2} \right)^2 + |\Delta_{\alpha}(\boldsymbol{k})|^2}. \tag{87}$$

This means we will still have chiral p-wave gap functions, as long as we let the BCS-interaction be defined in the Zeeman-modified helicity basis $d_{\boldsymbol{k},\alpha}$:

$$H_I = \sum_{\boldsymbol{k},\boldsymbol{k'},\boldsymbol{q}} \sum_{\alpha,\alpha',\beta,\beta'} V_{\alpha,\alpha',\beta,\beta'}(\boldsymbol{k},\boldsymbol{k'},\boldsymbol{q}) d^{\dagger}_{\boldsymbol{k},\alpha} d^{\dagger}_{-\boldsymbol{k}+\boldsymbol{q},\beta} d_{-\boldsymbol{k'}+\boldsymbol{q},\beta'} d_{\boldsymbol{k'},\alpha'}. \tag{88}$$

The arguments leading to equation (68) apply to this interaction in exactly the same way.

To find the spin basis interaction, we go through the reverse transformations, finding

$$\begin{aligned} H_I &= \sum_{\boldsymbol{k},\boldsymbol{k'},\boldsymbol{q}} \sum_{\alpha,\alpha',\beta,\beta'} V_{\alpha,\alpha',\beta,\beta'}(\boldsymbol{k},\boldsymbol{k'},\boldsymbol{q}) d^{\dagger}_{\boldsymbol{k},\alpha} d^{\dagger}_{-\boldsymbol{k}+\boldsymbol{q},\beta} d_{-\boldsymbol{k'}+\boldsymbol{q},\beta'} d_{\boldsymbol{k'},\alpha'} \\ &= \sum_{\boldsymbol{k},\boldsymbol{k'},\boldsymbol{q}} \sum_{\alpha,\alpha',\beta,\beta'} V_{\alpha,\alpha',\beta,\beta'}(\boldsymbol{k},\boldsymbol{k'},\boldsymbol{q}) (\cos(\theta_{\boldsymbol{k}}) a_{\boldsymbol{k},\alpha} + \Gamma_{2\bar{\alpha}} \sin(\theta_{\boldsymbol{k}}) a_{\boldsymbol{k},\bar{\alpha}}) (\cos(\theta_{-\boldsymbol{k}+\boldsymbol{q}}) a_{-\boldsymbol{k}+\boldsymbol{q},\beta} + \Gamma_{2\bar{\beta}} \sin(\theta_{-\boldsymbol{k}+\boldsymbol{q}}) a_{-\boldsymbol{k}+\boldsymbol{q},\bar{\beta}}) \\ &\qquad (\cos(\theta_{-\boldsymbol{k'}+\boldsymbol{q}}) a_{-\boldsymbol{k'}+\boldsymbol{q},\beta'} + \Gamma_{2\bar{\beta'}} \sin(\theta_{-\boldsymbol{k'}+\boldsymbol{q}}) a_{-\boldsymbol{k'}+\boldsymbol{q},\bar{\beta'}}) (\cos(\theta_{\boldsymbol{k'}}) a_{\boldsymbol{k'},\alpha'} + \Gamma_{2\bar{\alpha'}} \sin(\theta_{\boldsymbol{k'}}) a_{\boldsymbol{k'},\bar{\alpha'}}) \end{aligned} \tag{89}$$

$$\begin{aligned} H_I = \sum_{\boldsymbol{k},\boldsymbol{k'},\boldsymbol{q}} \sum_{\alpha,\alpha',\beta,\beta'} V_{\alpha,\alpha',\beta,\beta'}(\boldsymbol{k},\boldsymbol{k'},\boldsymbol{q}) (&\cos(\theta_{\boldsymbol{k}}) \cos(\theta_{-\boldsymbol{k}+\boldsymbol{q}}) \cos(\theta_{-\boldsymbol{k'}+\boldsymbol{q}}) \cos(\theta_{\boldsymbol{k'}}) a^{\dagger}_{\boldsymbol{k},\alpha} a^{\dagger}_{-\boldsymbol{k}+\boldsymbol{q},\beta} a_{-\boldsymbol{k'}+\boldsymbol{q},\beta'} a_{\boldsymbol{k'},\alpha'} \\ &+\Gamma_{2\bar{\alpha}} \sin(\theta_{\boldsymbol{k}}) \cos(\theta_{-\boldsymbol{k}+\boldsymbol{q}}) \cos(\theta_{-\boldsymbol{k'}+\boldsymbol{q}}) \cos(\theta_{\boldsymbol{k'}}) a^{\dagger}_{\boldsymbol{k},\bar{\alpha}} a^{\dagger}_{-\boldsymbol{k}+\boldsymbol{q},\beta} a_{-\boldsymbol{k'}+\boldsymbol{q},\beta'} a_{\boldsymbol{k'},\alpha'} \\ &+\Gamma_{2\bar{\beta}} \cos(\theta_{\boldsymbol{k}}) \sin(\theta_{-\boldsymbol{k}+\boldsymbol{q}}) \cos(\theta_{-\boldsymbol{k'}+\boldsymbol{q}}) \cos(\theta_{\boldsymbol{k'}}) a^{\dagger}_{\boldsymbol{k},\bar{\alpha}} a^{\dagger}_{-\boldsymbol{k}+\boldsymbol{q},\bar{\beta}} a_{-\boldsymbol{k'}+\boldsymbol{q},\beta'} a_{\boldsymbol{k'},\alpha'} \\ &+\ldots), \end{aligned} \tag{90}$$

where the sixteen terms in the parenthesis are not all written out for brevity. Since the sum runs over both bands in each index, we can reverse in every term the barred and unbarred indices in such a way that the field operators factor:

$$\begin{aligned} H_I = \sum_{\boldsymbol{k},\boldsymbol{k'},\boldsymbol{q}} \sum_{\alpha,\alpha',\beta,\beta'} (&V_{\alpha,\alpha',\beta,\beta'}(\boldsymbol{k},\boldsymbol{k'},\boldsymbol{q}) \cos(\theta_{\boldsymbol{k}}) \cos(\theta_{-\boldsymbol{k}+\boldsymbol{q}}) \cos(\theta_{-\boldsymbol{k'}+\boldsymbol{q}}) \cos(\theta_{\boldsymbol{k'}}) \\ &+\Gamma_{2\alpha} V_{\bar{\alpha},\alpha',\beta,\beta'}(\boldsymbol{k},\boldsymbol{k'},\boldsymbol{q}) \sin(\theta_{\boldsymbol{k}}) \cos(\theta_{-\boldsymbol{k}+\boldsymbol{q}}) \cos(\theta_{-\boldsymbol{k'}+\boldsymbol{q}}) \cos(\theta_{\boldsymbol{k'}}) \\ &+\Gamma_{2\beta} V_{\alpha,\alpha',\bar{\beta},\beta'}(\boldsymbol{k},\boldsymbol{k'},\boldsymbol{q}) \cos(\theta_{\boldsymbol{k}}) \sin(\theta_{-\boldsymbol{k}+\boldsymbol{q}}) \cos(\theta_{-\boldsymbol{k'}+\boldsymbol{q}}) \cos(\theta_{\boldsymbol{k'}}) \\ &+\ldots) a^{\dagger}_{\boldsymbol{k},\alpha} a^{\dagger}_{-\boldsymbol{k}+\boldsymbol{q},\beta} a_{-\boldsymbol{k'}+\boldsymbol{q},\beta'} a_{\boldsymbol{k'},\alpha'} \end{aligned} \tag{91}$$

This equation has the same form as equation (47), with a differing potential defined by the sixteen terms in the parenthesis above. Inserting we get

$$H_I = \sum_{\boldsymbol{k},\boldsymbol{k'},\boldsymbol{q}} \sum_{\alpha,\alpha',\beta,\beta'} V_{\alpha,\alpha',\beta,\beta'}(\boldsymbol{k},\boldsymbol{k'},\boldsymbol{q}) U^{s,s',\sigma,\sigma'}_{\alpha,\alpha',\beta,\beta'}(\boldsymbol{k},\boldsymbol{k'},\boldsymbol{q}) Z^\dagger_{s\alpha}(\boldsymbol{k}) Z^\dagger_{\sigma\beta}(-\boldsymbol{k}+\boldsymbol{q}) Z_{\sigma'\beta'}(-\boldsymbol{k'}+\boldsymbol{q}) Z_{s'\alpha'}(\boldsymbol{k'}) c^\dagger_{\boldsymbol{k},s} c^\dagger_{-\boldsymbol{k}+\boldsymbol{q},\sigma} c_{-\boldsymbol{k'}+\boldsymbol{q},\sigma'} c_{\boldsymbol{k'},s'}. \tag{92}$$

once again switching the barred indices with unbarred ones in each term as to factor out the potential $V_{\alpha,\alpha',\beta,\beta'}(\boldsymbol{k},\boldsymbol{k'},\boldsymbol{q})$, and then using that $\Gamma_{\alpha\bar{\beta}} = -\Gamma_{\alpha\beta}$ to find $Z_{s\bar{\alpha}}(\boldsymbol{k}) = \Gamma_{\uparrow s} Z_{s\alpha}(\boldsymbol{k})$. The sixteen term coefficient to the interaction becomes

$$\begin{aligned}
U^{s,s',\sigma,\sigma'}_{\alpha,\alpha',\beta,\beta'}(\boldsymbol{k},\boldsymbol{k'},\boldsymbol{q}) =& c_{\boldsymbol{k}} c_{-\boldsymbol{k}+\boldsymbol{q}} c_{-\boldsymbol{k'}+\boldsymbol{q}} c_{\boldsymbol{k'}} + s_{\boldsymbol{k}} c_{-\boldsymbol{k}+\boldsymbol{q}} c_{-\boldsymbol{k'}+\boldsymbol{q}} c_{\boldsymbol{k'}} \Gamma_{1\alpha}\Gamma_{\uparrow s} + c_{\boldsymbol{k}} s_{-\boldsymbol{k}+\boldsymbol{q}} c_{-\boldsymbol{k'}+\boldsymbol{q}} c_{\boldsymbol{k'}} \Gamma_{1\beta}\Gamma_{\uparrow\sigma} + c_{\boldsymbol{k}} c_{-\boldsymbol{k}+\boldsymbol{q}} s_{-\boldsymbol{k'}+\boldsymbol{q}} c_{\boldsymbol{k'}} \Gamma_{1\beta'}\Gamma_{\uparrow\sigma'} \\
&+ c_{\boldsymbol{k}} c_{-\boldsymbol{k}+\boldsymbol{q}} c_{-\boldsymbol{k'}+\boldsymbol{q}} s_{\boldsymbol{k'}} \Gamma_{1\alpha'}\Gamma_{\uparrow s'} + s_{\boldsymbol{k}} s_{-\boldsymbol{k}+\boldsymbol{q}} c_{-\boldsymbol{k'}+\boldsymbol{q}} c_{\boldsymbol{k'}} \Gamma_{\beta\alpha}\Gamma_{\sigma s} + c_{\boldsymbol{k}} c_{-\boldsymbol{k}+\boldsymbol{q}} s_{-\boldsymbol{k'}+\boldsymbol{q}} s\boldsymbol{k'} \Gamma_{\beta'\alpha'}\Gamma_{\sigma' s'} \\
&+ s_{\boldsymbol{k}} c_{-\boldsymbol{k}+\boldsymbol{q}} s_{-\boldsymbol{k'}+\boldsymbol{q}} c_{\boldsymbol{k'}} \Gamma_{\beta'\alpha}\Gamma_{\sigma' s} + s_{\boldsymbol{k}} c_{-\boldsymbol{k}+\boldsymbol{q}} c_{-\boldsymbol{k'}+\boldsymbol{q}} s_{\boldsymbol{k'}} \Gamma_{\alpha'\alpha}\Gamma_{s' s} + c_{\boldsymbol{k}} s_{-\boldsymbol{k}+\boldsymbol{q}} s_{-\boldsymbol{k'}+\boldsymbol{q}} c_{\boldsymbol{k'}} \Gamma_{\beta\beta'}\Gamma_{\sigma\sigma'} \\
&+ c_{\boldsymbol{k}} s_{-\boldsymbol{k}+\boldsymbol{q}} c_{-\boldsymbol{k'}+\boldsymbol{q}} s_{\boldsymbol{k'}} \Gamma_{\beta\alpha'}\Gamma_{\sigma s'} + s_{\boldsymbol{k}} c_{-\boldsymbol{k}+\boldsymbol{q}} s_{-\boldsymbol{k'}+\boldsymbol{q}} s_{\boldsymbol{k'}} \Gamma_{\beta'\alpha'}\Gamma_{\sigma' s'}\Gamma_{1\alpha}\Gamma_{\uparrow s} + c_{\boldsymbol{k}} s_{-\boldsymbol{k}+\boldsymbol{q}} s_{-\boldsymbol{k'}+\boldsymbol{q}} s_{\boldsymbol{k'}} \Gamma_{\beta'\alpha'}\Gamma_{\sigma' s'}\Gamma_{1\beta}\Gamma_{\uparrow\sigma} \\
&+ s_{\boldsymbol{k}} s_{-\boldsymbol{k}+\boldsymbol{q}} s_{-\boldsymbol{k'}+\boldsymbol{q}} c_{\boldsymbol{k'}} \Gamma_{\beta\alpha}\Gamma_{\sigma s}\Gamma_{1\beta'}\Gamma_{\uparrow\sigma'} + s_{\boldsymbol{k}} s_{-\boldsymbol{k}+\boldsymbol{q}} c_{-\boldsymbol{k'}+\boldsymbol{q}} s_{\boldsymbol{k'}} \Gamma_{\beta\alpha}\Gamma_{\sigma s}\Gamma_{1\alpha'}\Gamma_{\uparrow s'} \\
&+ s_{\boldsymbol{k}} s_{-\boldsymbol{k}+\boldsymbol{q}} s_{-\boldsymbol{k'}+\boldsymbol{q}} s_{\boldsymbol{k'}} \Gamma_{\beta\alpha}\Gamma_{\sigma s}\Gamma_{\beta'\alpha'}\Gamma_{\sigma' s'},
\end{aligned} \tag{93}$$

where we have made for notational simplicity the definitions $c_{\boldsymbol{k}} = \cos(\theta_{\boldsymbol{k}}), s_{\boldsymbol{k}} = \sin(\theta_{\boldsymbol{k}})$. Setting $B \to 0$ we see using equation (85) that $\theta_{\boldsymbol{k}} \to 0$, and so $U^{s,s',\sigma,\sigma'}_{\alpha,\alpha',\beta,\beta'}(\boldsymbol{k},\boldsymbol{k'},\boldsymbol{q}) \to 1$, and as expected equation (92) reduces to equation (49).

For zero in-plane fields, we have $|A_{\boldsymbol{k}}| = |A_{-\boldsymbol{k}}|$, and so $\sin(\theta_{\boldsymbol{k}}) = \sin(\theta_{-\boldsymbol{k}})$, $\cos(\theta_{\boldsymbol{k}}) = \cos(\theta_{-\boldsymbol{k}})$, and the above is simplified for $\boldsymbol{q} = 0$:

$$\begin{aligned}
U^{s,s',\sigma,\sigma'}_{\alpha,\alpha',\beta,\beta'}(\boldsymbol{k},\boldsymbol{k'},0) =& c^2_{\boldsymbol{k}} c^2_{\boldsymbol{k'}} + s_{\boldsymbol{k}} c_{\boldsymbol{k}} c^2_{\boldsymbol{k'}} (\Gamma_{1\alpha}\Gamma_{\uparrow s} + \Gamma_{1\beta}\Gamma_{\uparrow\sigma}) + c^2_{\boldsymbol{k}} c_{\boldsymbol{k'}} s_{\boldsymbol{k'}} (\Gamma_{1\alpha'}\Gamma_{\uparrow s'} + \Gamma_{1\beta'}\Gamma_{\uparrow\sigma'}) + c^2_{\boldsymbol{k}} s^2_{\boldsymbol{k'}} \Gamma_{\alpha'\beta'}\Gamma_{\sigma' s'} + s^2_{\boldsymbol{k}} c^2_{\boldsymbol{k'}} \Gamma_{\alpha\beta}\Gamma_{\sigma s} \\
&+ s_{\boldsymbol{k}} c_{\boldsymbol{k}} s_{\boldsymbol{k'}} c_{\boldsymbol{k'}} (\Gamma_{\alpha\beta'}\Gamma_{s\sigma'} + \Gamma_{\alpha'\beta}\Gamma_{s'\sigma} + \Gamma_{\alpha'\alpha}\Gamma_{ss'} + \Gamma_{\beta\beta'}\Gamma_{\sigma\sigma'}) + s_{\boldsymbol{k}} c_{\boldsymbol{k}} s^2_{\boldsymbol{k'}} \Gamma_{\beta'\alpha'}\Gamma_{\sigma' s'} (\Gamma_{1\alpha}\Gamma_{\uparrow s} + \Gamma_{1\beta}\Gamma_{\uparrow\sigma}) \\
&+ s^2_{\boldsymbol{k}} c_{\boldsymbol{k'}} s_{\boldsymbol{k'}} \Gamma_{\beta\alpha}\Gamma_{\sigma s} (\Gamma_{1\alpha'}\Gamma_{\uparrow s'} + \Gamma_{1\beta'}\Gamma_{\uparrow\sigma'}) + s^2_{\boldsymbol{k}} s^2_{\boldsymbol{k'}} \Gamma_{\beta'\alpha'}\Gamma_{\sigma' s'}\Gamma_{\beta\alpha}\Gamma_{\sigma s}.
\end{aligned} \tag{94}$$

Going back to equation (92) and inserting the potential (67) as an example, we see that each spin configuration contributes, since $U^{s,s',\sigma,\sigma'}_{\alpha,\alpha',\beta,\beta'}(\boldsymbol{k},\boldsymbol{k'},0)$ has terms that are antisymmetric in every possible combination of indices. Working out the specifics we see that

$$\begin{aligned}
H_I = \sum_{\boldsymbol{k},\boldsymbol{k'},s,s'} A_{\boldsymbol{k}} A^\dagger_{\boldsymbol{k'}} [& \Phi^\dagger_k \Phi_{\boldsymbol{k'}} \cos(2\theta_{\boldsymbol{k}}) \cos(2\theta_{\boldsymbol{k'}}) \Gamma_{ss'} c^\dagger_{\boldsymbol{k},s} c^\dagger_{-\boldsymbol{k},-s} c_{-\boldsymbol{k'},-s'} c_{\boldsymbol{k'},s'} \\
&+ (Z^\dagger_{s1}(\boldsymbol{k}))^2 (Z_{s'1}(\boldsymbol{k'}))^2 \sin(2\theta_{\boldsymbol{k}}) \sin(2\theta_{\boldsymbol{k'}}) c^\dagger_{\boldsymbol{k},s} c^\dagger_{-\boldsymbol{k},s} c_{-\boldsymbol{k'},s'} c_{\boldsymbol{k'},s'} \\
&+ \Phi^\dagger_{\boldsymbol{k}} (Z_{s'1}(\boldsymbol{k'}))^2 \cos(2\theta_{\boldsymbol{k}}) \sin(2\theta_{\boldsymbol{k'}}) \Gamma_{s1} c^\dagger_{\boldsymbol{k},-s} c^\dagger_{-\boldsymbol{k},s} c_{-\boldsymbol{k'},s'} c_{\boldsymbol{k'},s'} \\
&+ \Phi_{\boldsymbol{k'}} (Z_{s1}(\boldsymbol{k}))^2 \sin(2\theta_{\boldsymbol{k}}) \cos(2\theta_{\boldsymbol{k'}}) \Gamma_{1s'} c^\dagger_{\boldsymbol{k},s} c^\dagger_{-\boldsymbol{k},s} c_{-\boldsymbol{k'},s'} c_{\boldsymbol{k'},-s'}]
\end{aligned} \tag{95}$$

Using this result we as expected can return to the zero-B-field case, by setting $B \to 0$ which through equation (85) results in $\cos(2\theta_{\boldsymbol{k}}) = 1, \sin(2\theta_{\boldsymbol{k}}) = 0$, and we reduce to equation (72). Conversely, by setting $B >> |A|$, $\cos(2\theta_{\boldsymbol{k}}) \sim 0, \sin(2\theta_{\boldsymbol{k}}) \sim -1$, and the interaction reduces to

$$H_I = \sum_{\boldsymbol{k},\boldsymbol{k'},s,s'} |A_{\boldsymbol{k}}||A_{\boldsymbol{k'}}| \begin{pmatrix} \Phi_{\boldsymbol{k}}\Phi^\dagger_{\boldsymbol{k'}} & \Phi_{\boldsymbol{k}}\Phi_{\boldsymbol{k'}} \\ \Phi^\dagger_{\boldsymbol{k}}\Phi^\dagger_{\boldsymbol{k'}} & \Phi^\dagger_{\boldsymbol{k}}\Phi_{\boldsymbol{k'}} \end{pmatrix}_{s,s'} c^\dagger_{\boldsymbol{k},s} c^\dagger_{-\boldsymbol{k},s} c_{-\boldsymbol{k'},s'} c_{\boldsymbol{k'},s'}, \tag{96}$$

As in the zero magnetic field case, the magnitude of the potential reduces to $|\boldsymbol{k}||\boldsymbol{k'}|$ for the continuum limit. The complex phase difference between k_x and k_y is what causes this, which is the core quality of chiral p-wave pairing.

V. BCS WITH IN-PLANE MAGNETIC FIELD

In regards to the article in by Florian Loder, A. P. Kampf and Thilo kopp [1] who worked on a system with in-plane magnetic fields and SOC. The in-plane fields as written above will lead to finite pair momentum superconducting

states, depending on the field strength relative to SOC strength. This is what makes the problem complex, and below some of the calculations in [1] will be investigated, and we will find slightly different results which lead to a differing potential as well as altered gap equations.

The specific calculation of interest here is the one leading from equation <4> to equation <5> in [1]. They are repeated in this text as (97) and (98) respectively.

A. The results of Loder et al.

At first we will present the calculations of Loder et al. from equation <4> to equation <5>, and then look at the gap equations.

The interaction defined by equation <4> is a BCS type interaction in the spin basis,

$$H_I = -U \sum_{\boldsymbol{k},\boldsymbol{k'},\boldsymbol{q},s} c^\dagger_{\boldsymbol{k},s} c^\dagger_{-\boldsymbol{k}+\boldsymbol{q},-s} c_{-\boldsymbol{k'}+\boldsymbol{q},-s} c_{\boldsymbol{k'},s}, \tag{97}$$

where U is the magnitude of the interaction, equal to $\frac{V}{2N^2}$ in [1] but the exact value is mostly irrelevant for this comparison. The next step is applying the transformations (31), with $\Phi_{\boldsymbol{k}}$ defined as in (37). With this they arrive at equation <5>, which reads

$$H_I = U \sum_{\boldsymbol{k},\boldsymbol{k'},\boldsymbol{q}} \sum_{\alpha,\alpha',\beta,\beta'} \Gamma_{\beta,\beta'} (V_{even}(\boldsymbol{k},\boldsymbol{k'},\boldsymbol{q}) + V_{odd}(\boldsymbol{k},\boldsymbol{k'},\boldsymbol{q}))\ a^\dagger_{\boldsymbol{k},\alpha} a^\dagger_{-\boldsymbol{k}+q,\beta} a_{-\boldsymbol{k'}+q,\beta'} a_{\boldsymbol{k'},\alpha'}. \tag{98}$$

Where

$$V_\lambda(\boldsymbol{k},\boldsymbol{k'},\boldsymbol{q}) = g^*_\lambda(\boldsymbol{k},\boldsymbol{q}) g_\lambda(\boldsymbol{k'},\boldsymbol{q}) \tag{99}$$

and

$$g_\lambda(\boldsymbol{k},\boldsymbol{q}) \begin{cases} \frac{1}{2}(\Phi_{\boldsymbol{k}} + \Phi_{-\boldsymbol{k}+q}) & \text{if } \lambda = even \\ \frac{1}{2}(\Phi_{\boldsymbol{k}} - \Phi_{-\boldsymbol{k}+q}) & \text{if } \lambda = odd \end{cases}. \tag{100}$$

After rewriting $(V_{even}(\boldsymbol{k},\boldsymbol{k'},\boldsymbol{q}) + V_{odd}(\boldsymbol{k},\boldsymbol{k'},\boldsymbol{q}))$ to the phases $(\Phi_{\boldsymbol{k}}\Phi^\dagger_{\boldsymbol{k'}} + \Phi_{-\boldsymbol{k}+\boldsymbol{q}}\Phi^\dagger_{-\boldsymbol{k'}+\boldsymbol{q}})$, the interaction reduces to

$$\begin{aligned} H_I &= U \sum_{\boldsymbol{k},\boldsymbol{k'},\boldsymbol{q}} \sum_{\alpha,\alpha',\beta,\beta'} \Gamma_{\beta,\beta'} (\Phi_{\boldsymbol{k}}\Phi^\dagger_{\boldsymbol{k'}} + \Phi_{-\boldsymbol{k}+\boldsymbol{q}}\Phi^\dagger_{-\boldsymbol{k'}+\boldsymbol{q}})\ a^\dagger_{\boldsymbol{k},\alpha} a^\dagger_{-\boldsymbol{k}+\boldsymbol{q},\beta} a_{-\boldsymbol{k'}+\boldsymbol{q},\beta'} a_{\boldsymbol{k'},\alpha'} \\ &= U \sum_{\boldsymbol{k},\boldsymbol{k'},\boldsymbol{q}} \sum_{\alpha,\alpha',\beta,\beta'} \Phi_{\boldsymbol{k}}\Phi^\dagger_{\boldsymbol{k'}} (\Gamma_{\beta,\beta'} + \Gamma_{\alpha,\alpha'})\ a^\dagger_{\boldsymbol{k},\alpha} a^\dagger_{-\boldsymbol{k}+\boldsymbol{q},\beta} a_{-\boldsymbol{k'}+\boldsymbol{q},\beta'} a_{\boldsymbol{k'},\alpha'}, \end{aligned} \tag{101}$$

where on the second line we have used anticommutation, shifted $(\boldsymbol{k},\boldsymbol{k'}) \to (-\boldsymbol{k}+\boldsymbol{q}, -\boldsymbol{k'}+\boldsymbol{q})$ and renamed $(\alpha,\beta,\alpha',\beta') \to (\beta,\alpha,\beta',\alpha')$ in the second term of the parenthesis. This is done to compare more easily with results presented below.

By applying typical mean-field approximations, they arrive at equation <13>, which reads (by adding the constant term from mean-field as well as the Hermitian conjugate that they have not included) as

$$\begin{aligned} H_I = \sum_{\boldsymbol{k},\boldsymbol{q}} \quad & \tilde{\Delta}_{odd}(\boldsymbol{k},\boldsymbol{q})(a^\dagger_{\boldsymbol{k},1} a^\dagger_{-\boldsymbol{k}+\boldsymbol{q},1} - a^\dagger_{\boldsymbol{k},2} a^\dagger_{-\boldsymbol{k}+\boldsymbol{q},2}) + \tilde{\Delta}_{even}(\boldsymbol{k},\boldsymbol{q})(a^\dagger_{\boldsymbol{k},1} a^\dagger_{-\boldsymbol{k}+\boldsymbol{q},2} - a^\dagger_{\boldsymbol{k},2} a^\dagger_{-\boldsymbol{k}+\boldsymbol{q},1}) \\ & + \tilde{\Delta}^\dagger_{odd}(\boldsymbol{k},\boldsymbol{q})(a_{-\boldsymbol{k}+\boldsymbol{q},1} a_{\boldsymbol{k},1} - a_{-\boldsymbol{k}+\boldsymbol{q},2} a_{\boldsymbol{k},2}) + \tilde{\Delta}^\dagger_{even}(\boldsymbol{k},\boldsymbol{q})(a_{-\boldsymbol{k}+\boldsymbol{q},2} a_{\boldsymbol{k},1} - a_{-\boldsymbol{k}+\boldsymbol{q},1} a_{\boldsymbol{k},2}) - B_L(\boldsymbol{k},\boldsymbol{q}). \end{aligned} \tag{102}$$

The gap functions are

$$\tilde{\Delta}_{odd}(\boldsymbol{k},\boldsymbol{q}) = Ug_{odd}(\boldsymbol{k},\boldsymbol{q})\sum_{\boldsymbol{k'}} g^{\dagger}_{odd}(\boldsymbol{k'},\boldsymbol{q})[b_{11}(\boldsymbol{k'},\boldsymbol{q}) - b_{22}(\boldsymbol{k'},\boldsymbol{q})]$$
$$\tilde{\Delta}_{even}(\boldsymbol{k},\boldsymbol{q}) = Ug_{even}(\boldsymbol{k},\boldsymbol{q})\sum_{\boldsymbol{k'}} g^{\dagger}_{even}(\boldsymbol{k'},\boldsymbol{q})[b_{12}(\boldsymbol{k'},\boldsymbol{q}) - b_{21}(\boldsymbol{k'},\boldsymbol{q})]. \tag{103}$$

and the constant term is

$$B_L(\boldsymbol{k},\boldsymbol{q}) = \tilde{\Delta}_{odd}(\boldsymbol{k},\boldsymbol{q})[b^{\dagger}_{11}(\boldsymbol{k},\boldsymbol{q}) - b^{\dagger}_{22}(\boldsymbol{k},\boldsymbol{q})] + \tilde{\Delta}_{even}(\boldsymbol{k},\boldsymbol{q})[b^{\dagger}_{12}(\boldsymbol{k},\boldsymbol{q}) - b^{\dagger}_{21}(\boldsymbol{k},\boldsymbol{q})]. \tag{104}$$

Next they rewrite the Hamiltonian into matrix form, as

$$H = \sum_{\boldsymbol{k}} \eta^{\dagger}_{\boldsymbol{k}} \begin{pmatrix} \xi_{\boldsymbol{k},1} & 0 & \tilde{\Delta}_{odd}(\boldsymbol{k},\boldsymbol{q}_1) & \tilde{\Delta}_{even}(\boldsymbol{k},\boldsymbol{q}_1) & \tilde{\Delta}_{odd}(\boldsymbol{k},\boldsymbol{q}_2) & \tilde{\Delta}_{even}(\boldsymbol{k},\boldsymbol{q}_2) \\ 0 & \xi_{\boldsymbol{k},2} & -\tilde{\Delta}_{even}(\boldsymbol{k},\boldsymbol{q}_1) & -\tilde{\Delta}_{odd}(\boldsymbol{k},\boldsymbol{q}_1) & -\tilde{\Delta}_{even}(\boldsymbol{k},\boldsymbol{q}_2) & -\tilde{\Delta}_{odd}(\boldsymbol{k},\boldsymbol{q}_2) \\ \tilde{\Delta}^{\dagger}_{odd}(\boldsymbol{k},\boldsymbol{q}_1) & -\tilde{\Delta}^{\dagger}_{even}(\boldsymbol{k},\boldsymbol{q}_1) & -\xi_{-\boldsymbol{k}+\boldsymbol{q}_1,1} & 0 & 0 & 0 \\ \tilde{\Delta}^{\dagger}_{even}(\boldsymbol{k},\boldsymbol{q}_1) & -\tilde{\Delta}^{\dagger}_{odd}(\boldsymbol{k},\boldsymbol{q}_1) & 0 & -\xi_{-\boldsymbol{k}+\boldsymbol{q}_1,2} & 0 & 0 \\ \tilde{\Delta}^{\dagger}_{odd}(\boldsymbol{k},\boldsymbol{q}_2) & -\tilde{\Delta}^{\dagger}_{even}(\boldsymbol{k},\boldsymbol{q}_2) & 0 & 0 & -\xi_{-\boldsymbol{k}+\boldsymbol{q}_2,1} & 0 \\ \tilde{\Delta}^{\dagger}_{even}(\boldsymbol{k},\boldsymbol{q}_2) & -\tilde{\Delta}^{\dagger}_{odd}(\boldsymbol{k},\boldsymbol{q}_2) & 0 & 0 & 0 & -\xi_{-\boldsymbol{k}+\boldsymbol{q}_2,2} \end{pmatrix} \eta_{\boldsymbol{k}} - \sum_{\boldsymbol{q}_i} B_L(\boldsymbol{k},\boldsymbol{q}_i), \tag{105}$$

where the matrix can be extended to support any number of $\boldsymbol{q}$-values, and

$$\eta^{\dagger}_{\boldsymbol{k}} = (a^{\dagger}_{\boldsymbol{k}1}, a^{\dagger}_{\boldsymbol{k}2}, a_{-\boldsymbol{k}+\boldsymbol{q}_1,1}, a_{-\boldsymbol{k}+\boldsymbol{q}_1,2}, a_{-\boldsymbol{k}+\boldsymbol{q}_2,1}, a_{-\boldsymbol{k}+\boldsymbol{q}_2,2}). \tag{106}$$

This matrix must be diagonalized numerically to solve the gap equations, and we call the eigenvalues $\lambda_\rho(\boldsymbol{k})$, with ρ being an index running from 1 to 6, or more if there are more pair momenta included in the sum. Note that these eigenvalues are dependent on all the pair momenta in the sum over $\boldsymbol{q}$, but this dependency is not written down for notational simplicity. In diagonalizing, the Hamiltonian will turn to the form of a free Fermi gas,

$$H = \sum_{\boldsymbol{k},\rho}\left(\lambda_\rho(\boldsymbol{k})\gamma^{\dagger}_{\boldsymbol{k},\rho}\gamma_{\boldsymbol{k},\rho} - \sum_{\boldsymbol{q}_i} B_L(\boldsymbol{k},\boldsymbol{q}_i)\right) \tag{107}$$

which is then used to minimize the free energy, as before, in order to find the gap equations:

$$\frac{\partial F}{\partial\tilde{\Delta}_\lambda(\boldsymbol{k},\boldsymbol{q}_i)} = -\frac{1}{\beta}\frac{\partial}{\partial\tilde{\Delta}_\lambda(\boldsymbol{k},\boldsymbol{q}_i)}\sum_{\boldsymbol{k},\rho}\left(\log(1+e^{-\beta\lambda_\rho(\boldsymbol{k})}) + \log e^{-\beta B_L(\boldsymbol{k},\boldsymbol{q}_i)}\right). \tag{108}$$

Setting $\frac{\partial F}{\partial\tilde{\Delta}_\lambda(\boldsymbol{k},\boldsymbol{q}_i)} = 0$ to minimize:

$$\frac{\partial B_L(\boldsymbol{k},\boldsymbol{q}_i)}{\partial\tilde{\Delta}_\lambda(\boldsymbol{k},\boldsymbol{q}_i)} = \sum_\rho \frac{\partial\lambda_\rho(\boldsymbol{k})}{\partial\tilde{\Delta}_\lambda(\boldsymbol{k},\boldsymbol{q}_i)}\frac{e^{-\beta\lambda_\rho(\boldsymbol{k})}}{1+e^{-\beta\lambda_\rho(\boldsymbol{k})}}. \tag{109}$$

Using equation (104) and using $\Delta_{odd}(\boldsymbol{k},\boldsymbol{q})$ in the derivatives, we see

$$(b^{\dagger}_{11}(\boldsymbol{k},\boldsymbol{q}_i) - b^{\dagger}_{22}(\boldsymbol{k},\boldsymbol{q}_i)) = \sum_\rho \frac{\partial\lambda_\rho(\boldsymbol{k})}{\partial\Delta_{odd}(\boldsymbol{k},\boldsymbol{q}_i)}\frac{e^{-\beta\lambda_\rho(\boldsymbol{k})}}{1+e^{-\beta\lambda_\rho(\boldsymbol{k})}}, \tag{110}$$

while for $\Delta_{even}(\boldsymbol{k},\boldsymbol{q}_i)$ we get

$$(b_{12}^{\dagger}(\boldsymbol{k},\boldsymbol{q}_i) - b_{21}^{\dagger}(\boldsymbol{k},\boldsymbol{q}_i)) = \sum_{\rho} \frac{\partial\lambda_\rho(\boldsymbol{k})}{\partial\Delta_{even}(\boldsymbol{k},\boldsymbol{q}_i)} \frac{e^{-\beta\lambda_\rho(\boldsymbol{k})}}{1+e^{-\beta\lambda_\rho(\boldsymbol{k})}}. \tag{111}$$

Using the definitions from equation (103), the gap equations are

$$\tilde{\Delta}_{odd}^{\dagger}(\boldsymbol{k},\boldsymbol{q}_i) = g_{odd}^{\dagger}(\boldsymbol{k},\boldsymbol{q}_i) \sum_{\rho,\boldsymbol{k}'} \left(\frac{\partial\lambda_\rho(\boldsymbol{k}')}{\partial\tilde{\Delta}_{odd}(\boldsymbol{k}',\boldsymbol{q}_i)} g_{odd}(\boldsymbol{k}',\boldsymbol{q}_i) \frac{e^{-\beta\lambda_\rho(\boldsymbol{k}')}}{1+e^{-\beta\lambda_\rho(\boldsymbol{k}')}} \right), \tag{112}$$

$$\tilde{\Delta}_{even}^{\dagger}(\boldsymbol{k},\boldsymbol{q}_i) = g_{even}^{\dagger}(\boldsymbol{k},\boldsymbol{q}_i) \sum_{\rho,\boldsymbol{k}'} \left(\frac{\partial\lambda_\rho(\boldsymbol{k}')}{\partial\tilde{\Delta}_{even}(\boldsymbol{k}',\boldsymbol{q}_i)} g_{even}(\boldsymbol{k}',\boldsymbol{q}_i) \frac{e^{-\beta\lambda_\rho(\boldsymbol{k}')}}{1+e^{-\beta\lambda_\rho(\boldsymbol{k}')}} \right). \tag{113}$$

To solve them, we must numerically diagonalize the matrix of equation (105) to find the eigenvalues, as well as their derivatives with respect to the gaps.

B. Corrected results

We return to equation (97), and work through the transformations in detail. As shall be shown, the result differs from equation (98), and this impacts the gap equations.

In order to transform equation (97) more easily, we rewrite the transformations (32) to the following form:

$$c_{\boldsymbol{k},s} = \frac{a_{\boldsymbol{k},1} + s\ a_{\boldsymbol{k},2}}{\sqrt{2}e^{i\frac{(1-s)}{2}\gamma_{\boldsymbol{k}}}}, \tag{114}$$

where we have defined $\Phi_{\boldsymbol{k}} = e^{i\gamma_{\boldsymbol{k}}}$ and changed the spin index s to ± 1, identifying $+1$ with spin up, and -1 with spin down. Inserting this rewritten transformation into equation (97):

$$\begin{aligned} H_I = \frac{-U}{4} \sum_{\boldsymbol{k},\boldsymbol{k}',\boldsymbol{q},s} & (a_{\boldsymbol{k},1}^{\dagger} + s a_{\boldsymbol{k},2}^{\dagger})(a_{-\boldsymbol{k}+q,1}^{\dagger} - s a_{-\boldsymbol{k}+q,2}^{\dagger})(a_{-\boldsymbol{k}'+q,1} - s a_{-\boldsymbol{k}'+q,2})(a_{\boldsymbol{k}',1} + s a_{\boldsymbol{k}',2}) \\ & \times e^{\frac{i}{2}((1-s)\gamma_{\boldsymbol{k}} + (1+s)\gamma_{-\boldsymbol{k}+q} + (1+s)\gamma_{-\boldsymbol{k}'+q} - (1-s)\gamma_{\boldsymbol{k}'})}, \end{aligned} \tag{115}$$

which by defining

$$X_{s,\alpha} \begin{cases} 1 \text{ if } \alpha = 1 \\ s \text{ if } \alpha = 2 \end{cases} \tag{116}$$

reduces to

$$\begin{aligned} H_I &= \frac{-U}{4} \sum_{\boldsymbol{k},\boldsymbol{k}',\boldsymbol{q},s} \sum_{\alpha,\alpha',\beta,\beta'} X_{s,\alpha} X_{-s,\beta} X_{-s,\beta'} X_{s,\alpha'} e^{\frac{i}{2}((1-s)\gamma_{\boldsymbol{k}} + (1+s)\gamma_{-\boldsymbol{k}+\boldsymbol{q}} + (1+s)\gamma_{-\boldsymbol{k}'+\boldsymbol{q}} - (1-s)\gamma_{\boldsymbol{k}'})} a_{\boldsymbol{k},\alpha}^{\dagger} a_{-\boldsymbol{k}+\boldsymbol{q},\beta}^{\dagger} a_{-\boldsymbol{k}'+\boldsymbol{q},\beta'} a_{\boldsymbol{k}',\alpha'} \\ &= \frac{-U}{4} \sum_{\boldsymbol{k},\boldsymbol{k}',\boldsymbol{q}} \sum_{\alpha,\alpha',\beta,\beta'} (X_{1,\alpha} X_{-1,\beta} X_{-1,\beta'} X_{1,\alpha'} e^{i(\gamma_{-\boldsymbol{k}+\boldsymbol{q}} - \gamma_{-\boldsymbol{k}'+\boldsymbol{q}})} + X_{-1,\alpha} X_{1,\beta} X_{1,\beta'} X_{-1,\alpha'} e^{i(\gamma_{\boldsymbol{k}} - \gamma_{\boldsymbol{k}'})}) a_{\boldsymbol{k},\alpha}^{\dagger} a_{-\boldsymbol{k}+\boldsymbol{q},\beta}^{\dagger} a_{-\boldsymbol{k}'+\boldsymbol{q},\beta'} a_{\boldsymbol{k}',\alpha'} \\ &= \frac{-U}{4} \sum_{\boldsymbol{k},\boldsymbol{k}',\boldsymbol{q}} \sum_{\alpha,\alpha',\beta,\beta'} (\Gamma_{\beta,\beta'} \Phi_{-\boldsymbol{k}+\boldsymbol{q}} \Phi_{-\boldsymbol{k}'+\boldsymbol{q}}^{\dagger} + \Gamma_{\alpha,\alpha'}\ \Phi_{\boldsymbol{k}} \Phi_{\boldsymbol{k}'}^{\dagger}) a_{\boldsymbol{k},\alpha}^{\dagger} a_{-\boldsymbol{k}+\boldsymbol{q},\beta}^{\dagger} a_{-\boldsymbol{k}'+\boldsymbol{q},\beta'} a_{\boldsymbol{k}',\alpha'}. \end{aligned} \tag{117}$$

We can simplify the third line in equation (117) further by as before renaming $(\beta,\beta') \leftrightarrow (\alpha,\alpha')$, $(\boldsymbol{k},\boldsymbol{k}') \to (-\boldsymbol{k}+\boldsymbol{q}, -\boldsymbol{k}'+\boldsymbol{q})$ in the first term only, and then anticommuting the field operators in that term $a_{-\boldsymbol{k}+\boldsymbol{q},\beta}^{\dagger} a_{\boldsymbol{k},\alpha}^{\dagger} a_{\boldsymbol{k}',\alpha'} a_{-\boldsymbol{k}'+\boldsymbol{q},\beta'} = a_{\boldsymbol{k},\alpha}^{\dagger} a_{-\boldsymbol{k}+\boldsymbol{q},\beta}^{\dagger} a_{-\boldsymbol{k}'+\boldsymbol{q},\beta'} a_{\boldsymbol{k}',\alpha'}$, for the final interaction

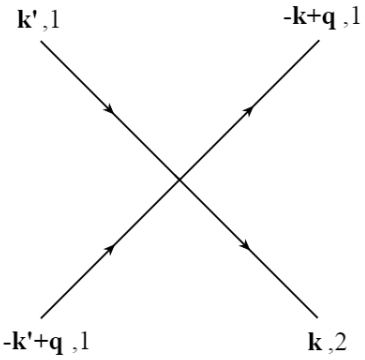

Figure 6: This diagram shows a type of interaction that is absent in the calculations from [1], and is present in the corrected Hamiltonian (118).

$$H_I = \frac{-U}{4} \sum_{\boldsymbol{k},\boldsymbol{k'},\boldsymbol{q}} \sum_{\alpha,\alpha',\beta,\beta'} 2\Gamma_{\alpha,\alpha'} \Phi_{\boldsymbol{k}} \Phi^\dagger_{\boldsymbol{k'}}\ a^\dagger_{\boldsymbol{k},\alpha} a^\dagger_{-\boldsymbol{k}+\boldsymbol{q},\beta} a_{-\boldsymbol{k'}+\boldsymbol{q},\beta'} a_{\boldsymbol{k'},\alpha'}. \tag{118}$$

This interaction is of a very similar form to equation (101), but with a clear and important difference. The coefficient in (101) is zero for certain band-index combinations such as $(\alpha, \beta, \beta', \alpha') = (1, 1, 1, 2)$, while the coefficient in (118) can only take on nonzero values. Hence (118) includes interactions such as the one shown in Figure 6. They are however identical for the remaining 8 combinations. Otherwise there is a difference in the prefactor which should not change the results significantly.

To see how this difference impacts the gap equations, we apply Mean-Field theory to the interaction in (118). Using the same definition as in equation (51) and the same general approach, we get

$$H_I = \frac{-U}{2} \sum_{\boldsymbol{k},\boldsymbol{k'},\boldsymbol{q}} \sum_{\alpha,\beta,\alpha',\beta'} \Gamma_{\alpha,\alpha'} \Phi_{\boldsymbol{k}} \Phi^\dagger_{\boldsymbol{k'}} [b^\dagger_{\alpha\beta}(\boldsymbol{k},\boldsymbol{q}) a_{-\boldsymbol{k'}+\boldsymbol{q},\beta'} a_{\boldsymbol{k'},\alpha'} + b_{\beta'\alpha'}(\boldsymbol{k'},\boldsymbol{q}) a^\dagger_{\boldsymbol{k},\alpha} a^\dagger_{-\boldsymbol{k}+\boldsymbol{q},\beta} - b^\dagger_{\alpha\beta}(\boldsymbol{k},\boldsymbol{q}) b_{\beta'\alpha'}(\boldsymbol{k'},\boldsymbol{q})]. \tag{119}$$

The following is simpler by substituting in the equation

$$\Phi_{\boldsymbol{k}} \Phi^\dagger_{\boldsymbol{k'}} = \sum_{\sigma,\lambda} g_\sigma(\boldsymbol{k},\boldsymbol{q}) g^\dagger_\lambda(\boldsymbol{k'},\boldsymbol{q}), \tag{120}$$

where the indices (λ, σ) are to be summed over $(even, odd)$. As is evident from their definition (100) $g_\lambda(\boldsymbol{k},\boldsymbol{q})$ is even or odd, depending on index, in the shift $\boldsymbol{k} \to -\boldsymbol{k} + \boldsymbol{q}$. Noting that the first term in equation (119) is just the hermitian conjugate of the second with some renaming of indices as it should be, we work on the second term:

$$\begin{aligned} &\sum_{\boldsymbol{k},\boldsymbol{k'},\boldsymbol{q}} \sum_{\alpha,\beta,\alpha',\beta'} \Gamma_{\alpha,\alpha'} \sum_{\sigma,\lambda} g_\sigma(\boldsymbol{k},\boldsymbol{q}) g^\dagger_\lambda(\boldsymbol{k'},\boldsymbol{q}) b_{\beta'\alpha'}(\boldsymbol{k'},\boldsymbol{q}) a^\dagger_{\boldsymbol{k},\alpha} a^\dagger_{-\boldsymbol{k}+\boldsymbol{q},\beta} \\ &= \sum_{\boldsymbol{k},\boldsymbol{k'},\boldsymbol{q}} \sum_{\alpha',\beta'} \sum_{\sigma,\lambda} \Gamma_{1,\alpha'} g_\sigma(\boldsymbol{k},\boldsymbol{q}) g^\dagger_\lambda(\boldsymbol{k'},\boldsymbol{q}) b_{\beta'\alpha'}(\boldsymbol{k'},\boldsymbol{q}) (a^\dagger_{\boldsymbol{k},1} a^\dagger_{-\boldsymbol{k}+\boldsymbol{q},1} - a^\dagger_{\boldsymbol{k},2} a^\dagger_{-\boldsymbol{k}+\boldsymbol{q},2} + a^\dagger_{\boldsymbol{k},1} a^\dagger_{-\boldsymbol{k}+\boldsymbol{q},2} - a^\dagger_{\boldsymbol{k},2} a^\dagger_{-\boldsymbol{k}+\boldsymbol{q},1}). \end{aligned} \tag{121}$$

The first two terms of field operators in this equation are both antisymmetric under the transformation $\boldsymbol{k} \to -\boldsymbol{k}+q$, while the sum of the two last terms are symmetric, as is evident by anticommutation. Thus we can rid ourselves of the corresponding symmetric and antisymmetric coefficients $g_\lambda(\boldsymbol{k},\boldsymbol{q})$, respectively for these field operator terms. This exact argument holds true in the same way when performing the sum over (α', β'), as $b_{11}(\boldsymbol{k'},\boldsymbol{q}) - b_{22}(\boldsymbol{k'},\boldsymbol{q})$ is antisymmetric and $b_{12}(\boldsymbol{k'},\boldsymbol{q}) - b_{21}(\boldsymbol{k'},\boldsymbol{q})$ is symmetric in the shift $\boldsymbol{k'} \to -\boldsymbol{k'} + \boldsymbol{q}$. Hence in these terms the symmetric and antisymmetric coefficients $g^\dagger_\lambda(\boldsymbol{k},\boldsymbol{q})$ also vanish, respectively. The $\boldsymbol{k'}$- and (α', β')-dependent quantities are subsumed into the gaps defined as

$$\Delta_{odd}(\boldsymbol{k},\boldsymbol{q}) = \frac{-U}{2} g_{odd}(\boldsymbol{k},\boldsymbol{q}) \sum_{\boldsymbol{k'}} g^{\dagger}_{odd}(\boldsymbol{k'},\boldsymbol{q})[b_{11}(\boldsymbol{k'},\boldsymbol{q}) - b_{22}(\boldsymbol{k'},\boldsymbol{q})] + g^{\dagger}_{even}(\boldsymbol{k'},\boldsymbol{q})[b_{21}(\boldsymbol{k'},\boldsymbol{q}) - b_{12}(\boldsymbol{k'},\boldsymbol{q})]$$

$$\Delta_{even}(\boldsymbol{k},\boldsymbol{q}) = \frac{-U}{2} g_{even}(\boldsymbol{k},\boldsymbol{q}) \sum_{\boldsymbol{k'}} g^{\dagger}_{odd}(\boldsymbol{k'},\boldsymbol{q})[b_{11}(\boldsymbol{k'},\boldsymbol{q}) - b_{22}(\boldsymbol{k'},\boldsymbol{q})] + g^{\dagger}_{even}(\boldsymbol{k'},\boldsymbol{q})[b_{21}(\boldsymbol{k'},\boldsymbol{q}) - b_{12}(\boldsymbol{k'},\boldsymbol{q})], \quad (122)$$

which, along with the constant term

$$B(\boldsymbol{k},\boldsymbol{q}) = \Delta_{odd}(\boldsymbol{k},\boldsymbol{q})[b^{\dagger}_{11}(\boldsymbol{k},\boldsymbol{q}) - b^{\dagger}_{22}(\boldsymbol{k},\boldsymbol{q})] + \Delta_{even}(\boldsymbol{k},\boldsymbol{q})[b^{\dagger}_{12}(\boldsymbol{k},\boldsymbol{q}) - b^{\dagger}_{21}(\boldsymbol{k},\boldsymbol{q})] \quad (123)$$

and the previous observation that the hermitian conjugate can be handled in the same way, leads to our interaction:

$$\begin{aligned} H_I = \sum_{\boldsymbol{k},q} \quad & \Delta_{odd}(\boldsymbol{k},\boldsymbol{q})(a^{\dagger}_{\boldsymbol{k},1}a^{\dagger}_{-\boldsymbol{k}+\boldsymbol{q},1} - a^{\dagger}_{\boldsymbol{k},2}a^{\dagger}_{-\boldsymbol{k}+\boldsymbol{q},2}) + \Delta_{even}(\boldsymbol{k},\boldsymbol{q})(a^{\dagger}_{\boldsymbol{k},1}a^{\dagger}_{-\boldsymbol{k}+\boldsymbol{q},2} - a^{\dagger}_{\boldsymbol{k},2}a^{\dagger}_{-\boldsymbol{k}+\boldsymbol{q},1}) \\ & + \Delta^{\dagger}_{odd}(\boldsymbol{k},\boldsymbol{q})(a_{-\boldsymbol{k}+\boldsymbol{q},1}a_{\boldsymbol{k},1} - a_{-\boldsymbol{k}+\boldsymbol{q},2}a_{\boldsymbol{k},2}) + \Delta^{\dagger}_{even}(\boldsymbol{k},\boldsymbol{q})(a_{-\boldsymbol{k}+\boldsymbol{q},2}a_{\boldsymbol{k},1} - a_{-\boldsymbol{k}+\boldsymbol{q},1}a_{\boldsymbol{k},2}) - B(\boldsymbol{k},\boldsymbol{q}), \end{aligned} \quad (124)$$

We see that there is a difference in gap structure, with the gaps (122) having extra cross terms $g_{odd}(\boldsymbol{k},\boldsymbol{q})g^{\dagger}_{even}(\boldsymbol{k'},\boldsymbol{q})$ and $g_{even}(\boldsymbol{k},\boldsymbol{q})g^{\dagger}_{odd}(\boldsymbol{k'},\boldsymbol{q})$ that the gaps (103) do not. However, the larger Hamiltonian structure is unchanged under this definition.

Since the overall structure of the Hamiltonian is unchanged, we may repeat the steps from equation (105) to equation (111), with new gaps $\Delta_{\lambda}(\boldsymbol{k},\boldsymbol{q})$ (and by extension, new constant term $B(\boldsymbol{k},\boldsymbol{q})$) now defined by equation (122). This time, we multiply (110) by $g^{\dagger}_{odd}(\boldsymbol{k'},\boldsymbol{q})\sum_{\boldsymbol{k}} g_{odd}(\boldsymbol{k},\boldsymbol{q})$ and (111) by $g^{\dagger}_{odd}(\boldsymbol{k'},\boldsymbol{q})\sum_{\boldsymbol{k}} g_{even}(\boldsymbol{k},\boldsymbol{q})$ and add them together, which with the new gaps yields

$$\Delta^{\dagger}_{odd}(\boldsymbol{k},\boldsymbol{q}) = g^{\dagger}_{odd}(\boldsymbol{k},\boldsymbol{q}) \sum_{\rho,k'} \left(\frac{\partial\lambda_{\rho}(\boldsymbol{k'})}{\partial\Delta_{odd}(\boldsymbol{k'},\boldsymbol{q})} g_{odd}(\boldsymbol{k'},\boldsymbol{q}) + \frac{\partial\lambda_{\rho}(\boldsymbol{k'})}{\partial\Delta_{even}(\boldsymbol{k'},\boldsymbol{q})} g_{even}(\boldsymbol{k'},\boldsymbol{q}) \right) \frac{e^{-\beta\lambda_{\rho}(\boldsymbol{k'})}}{1+e^{-\beta\lambda_{\rho}(\boldsymbol{k'})}}. \quad (125)$$

Multiplying instead by $g^{\dagger}_{even}(\boldsymbol{k'},\boldsymbol{q})\sum_{k} g_{odd}(\boldsymbol{k},\boldsymbol{q})$ and $g^{\dagger}_{even}(\boldsymbol{k'},\boldsymbol{q})\sum_{k} g_{even}(\boldsymbol{k},\boldsymbol{q})$:

$$\Delta^{\dagger}_{even}(\boldsymbol{k},\boldsymbol{q}) = g^{\dagger}_{even}(\boldsymbol{k},\boldsymbol{q}) \sum_{\rho,k'} \left(\frac{\partial\lambda_{\rho}(\boldsymbol{k'})}{\partial\Delta_{odd}(\boldsymbol{k'},\boldsymbol{q})} g_{odd}(\boldsymbol{k'},\boldsymbol{q}) + \frac{\partial\lambda_{\rho}(\boldsymbol{k'})}{\partial\Delta_{even}(\boldsymbol{k'},\boldsymbol{q})} g_{even}(\boldsymbol{k'},\boldsymbol{q}) \right) \frac{e^{-\beta\lambda_{\rho}(\boldsymbol{k'})}}{1+e^{-\beta\lambda_{\rho}(\boldsymbol{k'})}}. \quad (126)$$

These are the same equations as in (113), (112), but with additional cross terms $g^{\dagger}_{odd}(\boldsymbol{k},\boldsymbol{q})g_{even}(\boldsymbol{k'},\boldsymbol{q})$ and $g^{\dagger}_{even}(\boldsymbol{k},\boldsymbol{q})g_{odd}(\boldsymbol{k'},\boldsymbol{q})$. Any gaps that could satisfy (113) and (112) must necessarily be unable to satisfy (126) and (125), and hence despite the seemingly identical structure between (124) and (102), the numerical solutions should differ.

Next, it is of interest to see what kind of spin-basis interaction one would require in order to get to the same results as Loder et al. To achieve this, we transform their helicity space interaction, before mean field approximations, equation (101) back to spin space, using equation (49). Using as potential $V_{\alpha,\beta,\alpha',\beta'}(\boldsymbol{k},\boldsymbol{k'},\boldsymbol{q}) = \Phi_{\boldsymbol{k}}\Phi^{\dagger}_{\boldsymbol{k'}}(\Gamma_{\alpha,\alpha'} + \Gamma_{\beta,\beta'})$:

$$H_I = U \sum_{\boldsymbol{k},\boldsymbol{k'},\boldsymbol{q}} \sum_{\alpha,\alpha',\beta,\beta'} \sum_{s,s',\sigma,\sigma'} \frac{\Phi_{\boldsymbol{k}}\Phi^{\dagger}_{\boldsymbol{k'}}(\Gamma_{\alpha,\alpha'} + \Gamma_{\beta,\beta'})}{4} Z^{\dagger}_{s\alpha}(\boldsymbol{k}) Z^{\dagger}_{\sigma\beta}(-\boldsymbol{k}+\boldsymbol{q}) Z_{\sigma'\beta'}(-\boldsymbol{k'}+\boldsymbol{q}) Z_{s'\alpha'}(\boldsymbol{k'}) c^{\dagger}_{\boldsymbol{k},s} c^{\dagger}_{-\boldsymbol{k}+\boldsymbol{q},\sigma} c_{-\boldsymbol{k'}+\boldsymbol{q},\sigma'} c_{\boldsymbol{k'},s'}. \quad (127)$$

The terms with $\Gamma_{\alpha,\alpha'}$ are antisymmetric in (α,α') and symmetric in (β,β'). Hence the only nonzero spin configuration is $(s,\sigma,\sigma',s') = (\downarrow,\uparrow,\uparrow,\downarrow)$. Likewise, the terms with $\Gamma_{\beta,\beta'}$ are antisymmetric in (β,β') and symmetric in (α,α'), and their spin configuration becomes $(s,\sigma,\sigma',s') = (\uparrow,\downarrow,\downarrow,\uparrow)$. These spin configurations bring along the factors $\Phi^{\dagger}_{\boldsymbol{k}}\Phi_{\boldsymbol{k'}}\Gamma_{\alpha,\alpha'}$ and $\Phi^{\dagger}_{-\boldsymbol{k}+\boldsymbol{q}}\Phi_{-\boldsymbol{k'}+\boldsymbol{q}}\Gamma_{\beta,\beta'}$ respectively, cancelling the band index dependence in both cases, and in the first term only also cancels the momentum dependence. The spin space interaction then reads

$$H_I = U \sum_{\boldsymbol{k},\boldsymbol{k'},\boldsymbol{q}} \sum_s Y_s(\boldsymbol{k},\boldsymbol{k'},\boldsymbol{q}) c^\dagger_{\boldsymbol{k},-s} c^\dagger_{-\boldsymbol{k}+\boldsymbol{q},s} c_{-\boldsymbol{k'}+\boldsymbol{q},s} c_{\boldsymbol{k'},-s}, \tag{128}$$

with the definition of $Y_s(\boldsymbol{k},\boldsymbol{k'},\boldsymbol{q})$ as

$$Y_s(\boldsymbol{k},\boldsymbol{k'},\boldsymbol{q}) \begin{cases} 1 & \text{if } s = \uparrow \\ \Phi_{\boldsymbol{k}} \Phi^\dagger_{-\boldsymbol{k}+\boldsymbol{q}} \Phi^\dagger_{\boldsymbol{k'}} \Phi_{-\boldsymbol{k'}+\boldsymbol{q}} & \text{if } s = \downarrow. \end{cases} \tag{129}$$

This interaction is clearly momentum dependent, but is only slightly unlike equation (97). By comparison, inserting the potential $V_{\alpha,\beta,\alpha',\beta'}(\boldsymbol{k},\boldsymbol{k'},\boldsymbol{q}) = (\Gamma_{\beta,\beta'} \Phi_{-\boldsymbol{k}+\boldsymbol{q}} \Phi^\dagger_{-\boldsymbol{k'}+\boldsymbol{q}} + \Gamma_{\alpha,\alpha'} \Phi_{\boldsymbol{k}} \Phi^\dagger_{\boldsymbol{k'}})$ into equation (49) instead, we see that using the exact same arguments, the momentum dependent phases will cancel perfectly, and we return to equation (97). Note also that for the case when the in-plane magnetic field is zero, $\Phi_{\boldsymbol{k}} = -\Phi_{-\boldsymbol{k}}$ and so $Y_s(\boldsymbol{k},\boldsymbol{k'},0) = 1$. In this case then equation (128) reduces to equation (97) for $\boldsymbol{q} = 0$, the dominant contribution, as we would expect from the fact that under these conditions equations (101) and (118) are also equivalent.

VI. SUMMARY

A model for cooper pairing in a square 2-dimensional lattice was established with both Rashba spin-orbit coupling and perpendicular Zeeman field. The cooper pairing interaction was defined in the set of eigenstates of the system after having included both SOC and Zeeman interactions, so as to more easily find conditions for chiral p-wave gap states. A specific cooper pairing potential $V_{\alpha,\alpha',\beta,\beta'}(\boldsymbol{k},\boldsymbol{k'},\boldsymbol{q}) = \Gamma_{\alpha,\alpha'} \delta_{\alpha\beta} \delta_{\alpha'\beta'} A_{\boldsymbol{k}} A^\dagger_{\boldsymbol{k'}}$ was used knowing that it leads to regular intraband pairing, as well as pair hopping between bands. These were chosen because they allow for zero center of mass momentum q as the most significant contribution to the Hamiltonian, thus simplifying the calculations. Under these conditions, the potential can be chosen to yield chiral p-wave structure in the gap equations, $\Delta_\alpha(\boldsymbol{k}) = \Delta_\alpha(\sin(k_y) + i\sin(k_x))$. We also established what the structure of the pairing interaction in spin-momentum space would have to be to acquire a given interaction in helicity band space, both with and without Zeeman field interactions. Using this, a spin-momentum interaction that would cause chiral p-wave pairing states was found.

The requirement for chiral p-wave gap states for the SOC states ends up being quite pleasing, with only a simple dependence on both spin and momentum. However, turning on the out of plane magnetic field and going to SOC + Zeeman states makes the spin-momentum interaction much more complex. This is somewhat unfortunate as the Zeeman field is important for raising one band out of the Fermi level so that the resulting Majorana fermions do not cancel out.

Further work of interest could be repeating the same calculations for different lattices, as this would impact the kinetic and SOC terms, and thus significantly change the resulting interactions leading to chiral p-wave. Generalizing equation (49) to include other kinds of interactions might be of interest, although using it to find chiral p-wave structures would also require generalizing the energy spectra and the gap equations themselves.

As for the calculation of in-plane fields, we found slightly differing transformations to that of [34], and further work on this would be of interest, to find the cause of this difference. The calculation of the BCS-interaction itself, going from spin-momentum eigenstates to helicity eigenstates, was repeated here as it was done in [1]. We found a discrepancy in the results that take the form of additional terms in the gap coefficients, but without changing the major structure of the equations. This difference in gap structure however does correspond to a difference in the gap equations themselves, which as explained above means that the numerical results found by Loder et al. should not solve the gap equations presented here.

Further work would involve investigating the numerical results more thoroughly to determine whether the large scale qualitative effects are changed by the correction of this interaction.

Appendix A: Cooper pair problem

In this appendix we will go through the beginnings of the cooper pair problem for finite in-plane and zero out of plane magnetic fields. We compare briefly with the appendix of [34]. The reason for these calculations is intrinsically

to find pair momenta that maximize the gaps, however doing this without approximations such as large in-plane fields is complex.

We first try a general Hamiltonian

$$H = \sum_{\boldsymbol{k}} \epsilon_{\boldsymbol{k}} a^\dagger_{\boldsymbol{k}} a_{\boldsymbol{k}} + \sum_{\boldsymbol{k},\boldsymbol{k'}} (V g_{\boldsymbol{k}} g^\dagger_{\boldsymbol{k'}}) a^\dagger_{\boldsymbol{k}} a^\dagger_{-\boldsymbol{k}} a_{-\boldsymbol{k'}} a_{\boldsymbol{k'}} \tag{A1}$$

with no band indices, zero COMM and a separable BCS interaction potential. The function $g_{\boldsymbol{k}}$ is arbitrary, and $\epsilon_{\boldsymbol{k}}$ is the one-particle energy of a particle with momentum k. Solving the Cooper pair problem involves solving the Schrödinger equation

$$H \left|\Psi\right\rangle = E_c \left|\Psi\right\rangle . \tag{A2}$$

We expand the state $\left|\Psi\right\rangle$ into a complete set of basis states

$$\left|\Psi\right\rangle = \sum_{\boldsymbol{p}} c_{\boldsymbol{p}} \left|\boldsymbol{p}, -\boldsymbol{p}\right\rangle \tag{A3}$$

and project down to $\langle \boldsymbol{p'}, -\boldsymbol{p'}| = |\boldsymbol{p'}, -\boldsymbol{p'}\rangle^\dagger$. This yields

$$(\epsilon_{\boldsymbol{p'}} + \epsilon_{-\boldsymbol{p'}} - E) c_{\boldsymbol{p'}} = -V \sum_{\boldsymbol{p}} c_{\boldsymbol{p}} g_{\boldsymbol{p'}} g^\dagger_{\boldsymbol{p}}. \tag{A4}$$

Next we look at the Cooper pairing problem for a general Hamiltonian with band indices and finite COMM q. This time the Hamiltonian is

$$H_0 + H_I = \sum_{\boldsymbol{k},\alpha} E_{\boldsymbol{k},\alpha} a^\dagger_{\boldsymbol{k},\alpha} a_{\boldsymbol{k},\alpha} + \sum_{\boldsymbol{k},\boldsymbol{k'}} \sum_{\alpha,\alpha',\beta,\beta',\gamma'} V_{\alpha,\alpha'}(\boldsymbol{k},\boldsymbol{k'},\boldsymbol{q}_{\gamma'}) a^\dagger_{\boldsymbol{k}+\frac{\boldsymbol{q}_{\gamma'}}{2},\alpha} a^\dagger_{-\boldsymbol{k}+\frac{\boldsymbol{q}_{\gamma'}}{2},\beta} a_{-\boldsymbol{k}+\frac{\boldsymbol{q}_{\gamma'}}{2},\beta'} a_{\boldsymbol{k}+\frac{\boldsymbol{q}_{\gamma'}}{2},\alpha'}. \tag{A5}$$

The potential is the same as for (118),

$$V_{\alpha,\alpha'}(\boldsymbol{k},\boldsymbol{k'},\boldsymbol{q}_{\gamma'}) = 2U\Gamma_{\alpha,\alpha'} \Phi_{\boldsymbol{k}+\frac{\boldsymbol{q}_\gamma}{2}} \Phi^\dagger_{\boldsymbol{k'}+\frac{\boldsymbol{q}_\gamma}{2}} \tag{A6}$$

with $\Phi_{\boldsymbol{k}}$ defined as (37). We expand this time $\left|\Psi\right\rangle$ as

$$\left|\Psi\right\rangle = \sum_{\boldsymbol{p},\gamma} c_\gamma(\boldsymbol{p},\boldsymbol{q}_\gamma) \left|\boldsymbol{p}+\frac{\boldsymbol{q}_\gamma}{2}, -\boldsymbol{p}+\frac{\boldsymbol{q}_\gamma}{2}\right\rangle_{\gamma,\gamma} \tag{A7}$$

The Cooper pair states are $\left|\boldsymbol{p}+\frac{\boldsymbol{q}_\gamma}{2}, -\boldsymbol{p}+\frac{\boldsymbol{q}_\gamma}{2}\right\rangle_{\gamma,\gamma} = a^\dagger_{\boldsymbol{p}+\frac{\boldsymbol{q}_\gamma}{2},\gamma} a^\dagger_{-\boldsymbol{p}+\frac{\boldsymbol{q}_\gamma}{2},\gamma} \left|0\right\rangle$. We expand this way because we are interested in pair hopping and intraband pairing, which are both covered by this expansion. The COMM $\boldsymbol{q}_\gamma$ are chosen such that they optimize pairing on band γ. In this case we only have one COMM for each band.

$$H_0 \left|\Psi\right\rangle = \sum_{\boldsymbol{k},\gamma} (E_{\boldsymbol{k}+\frac{\boldsymbol{q}_\gamma}{2},\gamma} + E_{-\boldsymbol{k}+\frac{\boldsymbol{q}_\gamma}{2},\gamma}) c_\gamma(\boldsymbol{k},\boldsymbol{q}_\gamma) \left|\boldsymbol{k}+\frac{\boldsymbol{q}_\gamma}{2}, -\boldsymbol{k}+\frac{\boldsymbol{q}_\gamma}{2}\right\rangle_{\gamma,\gamma} \tag{A8}$$

$$H_I \left|\Psi\right\rangle = \sum_{\boldsymbol{k},\boldsymbol{p}} \sum_{\alpha,\beta,\gamma,\gamma'} V_{\alpha,\gamma}(\boldsymbol{k},\boldsymbol{p},\boldsymbol{q}_{\gamma'}) c_\gamma(\boldsymbol{p},\boldsymbol{q}_\gamma) \left|\boldsymbol{k}+\frac{\boldsymbol{q}_{\gamma'}}{2}, -\boldsymbol{k}+\frac{\boldsymbol{q}_{\gamma'}}{2}\right\rangle_{\alpha,\beta} \tag{A9}$$

$$E_{c,\boldsymbol{q}} \left|\Psi\right\rangle = E_{c,\boldsymbol{q}} \sum_{\boldsymbol{p},\gamma} c_\gamma(\boldsymbol{p},\boldsymbol{q}_\gamma) \left|\boldsymbol{p}+\frac{\boldsymbol{q}_\gamma}{2}, -\boldsymbol{p}+\frac{\boldsymbol{q}_\gamma}{2}\right\rangle_{\gamma,\gamma} \tag{A10}$$

We multiply the Schrödinger equation (A2) by $\langle \boldsymbol{k}' + \frac{\boldsymbol{q}_\sigma}{2}, -\boldsymbol{k}' + \frac{\boldsymbol{q}_\sigma}{2}|_{\sigma,\sigma}$ from the left:

$$(E_{\boldsymbol{k}'+\frac{\boldsymbol{q}_\sigma}{2},\sigma} + E_{-\boldsymbol{k}'+\frac{\boldsymbol{q}_\sigma}{2},\sigma})c_\sigma(\boldsymbol{k}', \boldsymbol{q}_\sigma) + \sum_{\boldsymbol{p},\gamma} V_{\sigma,\gamma}(\boldsymbol{k}', \boldsymbol{p}, \boldsymbol{q}_\sigma))c_\gamma(\boldsymbol{p}, \boldsymbol{q}_\gamma) = E_{c,\boldsymbol{q}} c_\sigma(\boldsymbol{k}', \boldsymbol{q}_\sigma) \tag{A11}$$

Using as potential $V_{\sigma,\gamma}(\boldsymbol{k}', \boldsymbol{p}, \boldsymbol{q}_\sigma) = U 2\Gamma_{\sigma\gamma}\Phi_{\boldsymbol{k}'+\frac{\boldsymbol{q}_\sigma}{2}}\Phi^\dagger_{\boldsymbol{p}+\frac{\boldsymbol{q}_\sigma}{2}}$, and defining $\Delta_\sigma(\boldsymbol{k}', \boldsymbol{q}_\sigma) = (E_{\boldsymbol{k}'+\frac{\boldsymbol{q}_\sigma}{2},\sigma} + E_{-\boldsymbol{k}'+\frac{\boldsymbol{q}_\sigma}{2},\sigma}) - E_{c,\boldsymbol{q}}$, we have

$$\Delta_\sigma(\boldsymbol{k}', \boldsymbol{q}_\sigma)c_\sigma(\boldsymbol{k}', \boldsymbol{q}_\sigma) = -\sum_{\boldsymbol{p},\gamma} 2U\Gamma_{\sigma\gamma}\Phi_{\boldsymbol{k}'+\frac{\boldsymbol{q}_\sigma}{2}}\Phi^\dagger_{\boldsymbol{p}+\frac{\boldsymbol{q}_\sigma}{2}} c_\gamma(\boldsymbol{p}, \boldsymbol{q}_\gamma) \tag{A12}$$

This equation can be compared to <A4> in [34]. To proceed, one would have to expand the wave functions $c_\sigma(\boldsymbol{k}', \boldsymbol{q}_\sigma)$ and interactions in square lattice harmonics, and then go to energy space and perform an integration.

[1] F. Loder, A. P. Kampf, and T. Kopp, Journal of Physics: Condensed Matter **25**, 362201 (2013).
[2] J. R. Schrieffer, *Theory of Superconductivity*, 4th ed. (Addison-Wesley, 1964).
[3] A. P. Schnyder, S. Ryu, A. Furusaki, and A. W. W. Ludwig, Phys. Rev. B **78**, 195125 (2008), arXiv:0803.2786v3.
[4] R. Roy, ArXiv e-prints (2008), arXiv:0803.2868.
[5] X.-L. Qi, T. L. Hughes, and S.-C. Zhang, Phys. Rev. B **78**, 195424 (2008).
[6] C. L. Kane and E. J. Mele, Phys. Rev. Lett. **95**, 226801 (2005).
[7] C. L. Kane and E. J. Mele, Phys. Rev. Lett. **95**, 146802 (2005).
[8] J. S. et al., PhysRevLett **92**, 126603 (2004).
[9] M. Z. Hasan and C. L. Kane, Rev. Mod. Phys. **82**, 3045–3067 (2010).
[10] X.-G. Wen, Adv. Phys.. **44**, 405 (1995), arXiv:cond-mat/9506066v2.
[11] D. J. Thouless, M. Kohmoto, M. P. Nightingale, and M. den Nijs, Phys. Rev. Lett. **49**, 405 (1982).
[12] Y. Hatsugai, Phys. Rev. Lett. **71**, 3697 (1993).
[13] M. KOHMOTO, ANNALS OF PHYSICS **160**, 343 (1985).
[14] C. Wu, B. A. Bernevig, and S.-C. Zhang, Phys. Rev. Lett. **96**, 106401 (2006).
[15] B. I. Halperin, Phys. Rev. B **25**, 2185 (1982).
[16] C. Xu and J. E. Moore, Phys. Rev. B **73**, 045322 (2006).
[17] X.-L. Qi and S.-C. Zhang, PhysRevLett (2010), 10.1103/PhysRevC.81.034903, arXiv:1008.2026v1.
[18] N. Read and D. Green, Phys. Rev. B **61**, 10267 (2000).
[19] C. Nayak, S. H. Simon, A. Stern, M. Freedman, and S. Das Sarma, Rev. Mod. Phys. **80**, 1083 (2008).
[20] J. D. Sau, R. M. Lutchyn, S. Tewari, and S. Das Sarma, Phys. Rev. Lett. **104**, 040502 (2010).
[21] M. Sato, Y. Takahashi, and S. Fujimoto, Phys. Rev. Lett. **103**, 020401 (2009).
[22] G. E. Volovik, Journal of Experimental and Theoretical Physics Letters **70**, 609 (1999).
[23] D. A. Ivanov, Phys. Rev. Lett. **86**, 268 (2001).
[24] A. P. Mackenzie and Y. Maeno, Rev. Mod. Phys. **75**, 657 (2003).
[25] X.-L. Qi, T. L. Hughes, and S.-C. Zhang, Phys. Rev. B **82**, 184516 (2010), arXiv:1003.5448 [cond-mat.mes-hall].
[26] Y. A. Bychkov and E. I. Rashba, Journal of Physics C: Solid State Physics **17**, 6039 (1984).
[27] V. Barzykin and L. P. Gor'kov, Phys. Rev. Lett. **89**, 227002 (2002).
[28] Z. Zheng, M. Gong, X. Zou, C. Zhang, and G. Guo, Phys. Rev. A **87**, 031602 (2013).
[29] F. Wu, G.-C. Guo, W. Zhang, and W. Yi, Phys. Rev. Lett. **110**, 110401 (2013).
[30] P. Fulde and R. A. Ferrell, Phys. Rev. **135**, A550 (1964).
[31] A. I. Larkin and Y. N. Ovchinnikov, Sov. Phys. JETP **20**, 762 (1965).
[32] C. Qu, Z. Zheng, M. Gong, Y. Xu, L. Mao, X. Zou, G. Guo, and C. Zhang, Nat Commun **4** (2013), article.
[33] W. Zhang and W. Yi, Nat Commun **4** (2013), article.
[34] E. Lake, C. Webb, D. A. Pesin, and O. A. Starykh, Phys. Rev. B **93**, 214516 (2016).
[35] P. Morel and P. W. Anderson, Phys. Rev. **125**, 1263 (1962).